REPORT DOCUMENTATION PAGE

Form Approved
OMB No. 074-0188

1. AGENCY USE ONLY (Leave blank)	2. REPORT DATE	3. REPORT TYPE AND DATE COVERED
	6 May 2008	

4. TITLE AND SUBTITLE
An Experimental Study of Water Injection into a Rolls-Royce Model 250-C20B Turboshaft Gas Turbine

5. FUNDING NUMBERS

6. AUTHOR(S)

Golden, Daniel L.

7. PERFORMING ORGANIZATION NAME(S) AND ADDRESS(ES)

8. PERFORMING ORGANIZATION REPORT NUMBER

9. SPONSORING/MONITORING AGENCY NAME(S) AND ADDRESS(ES)

US Naval Academy
Annapolis, MD 21402

10. SPONSORING/MONITORING AGENCY REPORT NUMBER

Trident Scholar project report no. 367 (2008)

11. SUPPLEMENTARY NOTES

12a. DISTRIBUTION/AVAILABILITY STATEMENT
This document has been approved for public release; its distribution is UNLIMITED.

12b. DISTRIBUTION CODE

13. ABSTRACT Environmental responsibility is a focus of researchers in many fields. In the field of engine and propulsion research this is manifested in a focus on minimization of emissions while maximizing efficiency and performance. Water Fog Injection (WFI) has been suggested as a method for the suppression of nitrous oxide emissions in gas turbines. WFI consists of spraying a fine mist of water into the compressor inlet of the gas turbine. Prior research on larger, higher pressure ratio engines determined the WFI can not only reduce nitrous oxide emissions but also yields increases in power output and thermodynamic efficiency. While previous research has focused on large gas turbines, the effects of water fog injection on a smaller, lower pressure ratio gas turbine, as represented by the Rolls-Royce Model 250-C20B, have yet to provide conclusive results. This investigation determined the effect of WFI on the Model 250-C20B's exhaust gas composition, power output, thermodynamic efficiency and component efficiencies. The investigation used an instrumented Model 250-C20B gas turbine and an original water spray system. Temperatures and pressures were measured for each of the gas turbine's five state points. Exhaust gas composition and output shaft torque and speed were also measured. Experiments were conducted with water fog injection water flow rates ranging from 0.1 to 1.4 gallons per minute. This represents up to a maximum of 5 percent of the maximum mass flow rate of air through the engine. The results of these tests were compared with baseline runs conducted with no water fog injection. From the experimental data it was determined that the exhaust gas composition was significantly affected by the water fog injection. (cont on p.2)

14. SUBJECT TERMS
gas turbine engine, water fog injection, cycle improvement, nitrous oxides

15. NUMBER OF PAGES
78

16. PRICE CODE

17. SECURITY CLASSIFICATION OF REPORT	18. SECURITY CLASSIFICATION OF THIS PAGE	19. SECURITY CLASSIFICATION OF ABSTRACT	20. LIMITATION OF ABSTRACT

Abstract

Environmental responsibility is a focus of researchers in many fields. In the field of engine and propulsion research this is manifested in a focus on minimization of emissions while maximizing efficiency and performance. Water Fog Injection (WFI) has been suggested as a method for the suppression of nitrous oxide emissions in gas turbines. WFI consists of spraying a fine mist of water into the compressor inlet of the gas turbine. Prior research on larger, higher pressure ratio engines determined the WFI can not only reduce nitrous oxide emissions but also yields increases in power output and thermodynamic efficiency. While previous research has focused on large gas turbines, the effects of water fog injection on a smaller, lower pressure ratio gas turbine, as represented by the Rolls-Royce Model 250-C20B, have yet to provide conclusive results.

This investigation determined the effect of WFI on the Model 250-C20B's exhaust gas composition, power output, thermodynamic efficiency and component efficiencies. The investigation used an instrumented Model 250-C20B gas turbine and an original water spray system. Temperatures and pressures were measured for each of the gas turbine's five state points. Exhaust gas composition and output shaft torque and speed were also measured. Experiments were conducted with water fog injection water flow rates ranging from 0.1 to 1.4 gallons per minute. This represents up to a maximum of 5 percent of the maximum mass flow rate of air through the engine. The results of these tests were compared with baseline runs conducted with no water fog injection.

From the experimental data it was determined that the exhaust gas composition was significantly affected by the water fog injection. The increase of WFI decreased the

concentration of nitrous oxides in the exhaust. NO_x concentration at 1.4 gallons per minute of WFI at maximum throttle setting was 27 percent of the concentration of NOx with no WFI. Also there was only a slight increase in the concentration of unburned hydrocarbons in the exhaust as the flow rate of the WFI was increased.

The effects of WFI on the power output of the engine were also determined to be significant. WFI increased the net power for a specified mass flow rate of air. However, the fuel flow rate of the engine was mechanically limited by the engine. This limited the maximum attainable net power with elevated WFI rates. Additionally, the Brake Specific Fuel Consumption of the engine increased as WFI rate increased. This indicated that though WFI increased power, it did so at the cost of elevated fuel consumption meaning the engine was less efficient.

These results are significant in that they define the practical limits of Water Fog Injection's efficacy for smaller gas turbines as represented by the Model 250-C20B. To a limited WFI water flow rate, it is possible to realize decreases in nitrous oxide emission and increases in power output over the baseline.

Keywords:

gas turbine engine, water fog injection, cycle improvement, nitrous oxides

Acknowledgments:

The Office of Naval Research
The Trident Scholar Committee
Mr. Charles Baesch, E&W Technical Support Department
Mr. John Hein, E&W Technical Support Department
Mr. Charlie Popp, E&W Technical Support Department

Table of Contents

List of Figures

List of Tables

I. Introduction and Background

Gas turbines play important roles in the military and civilian sectors. They provide electrical power and propulsion for numerous vehicles including armored vehicles, ships, and aircraft. Technological advancements in the gas turbine have greatly enhanced the capabilities of the Navy by enabling ships and aircraft to take advantage of high power engines at a reduced weight penalty.

A basic turboshaft gas turbine engine is comprised of a compressor, a combustion chamber, a gas generator turbine, and a power turbine. The gas turbine engine operates on the principle that a working fluid, air, is compressed, is heated by the combustion of fuel, and then converts this energy to useful power mechanically in an expansion process. A schematic of a basic turboshaft gas turbine can be found in Figure 1. A gas turbine engine can be an open cycle system, meaning that the working fluid is exhausted to the atmosphere, not recycled; however its operation can be modeled using a closed thermodynamic cycle pioneered by George Brayton.

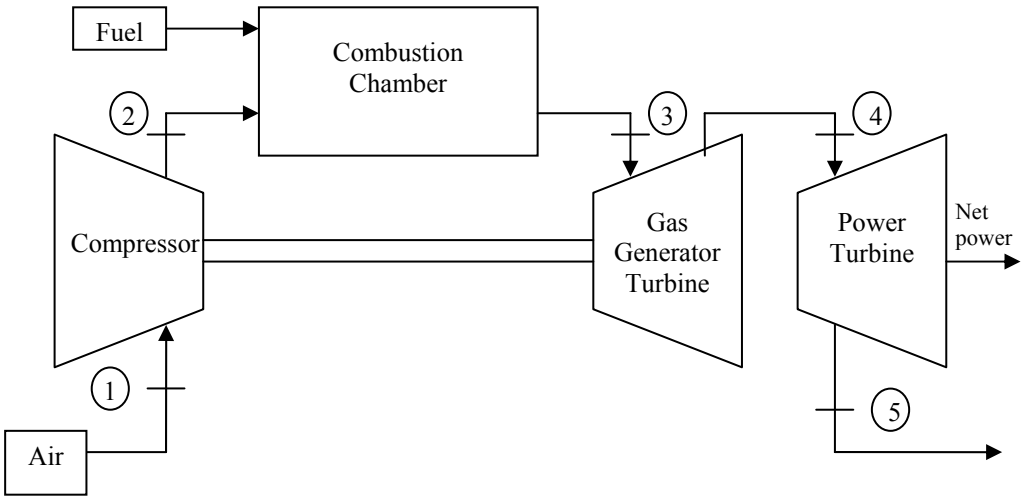

Figure 1 Schematic of a Turboshaft Gas Turbine Engine

The working fluid of the Brayton cycle, like an actual gas turbine, is typically air. The components of the Brayton cycle, though, are different. The Brayton cycle replaces the combustion chamber and fuel with a heat exchanger and heat addition. It replaces the exhaust process with another heat exchanger and heat rejection. A schematic of the basic Brayton cycle is shown in Figure 2.

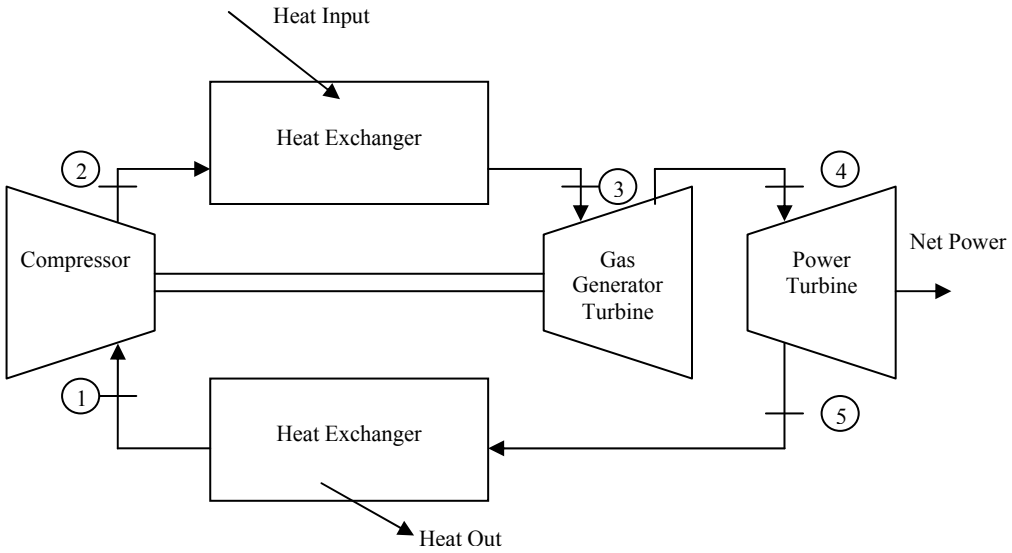

Figure 2 A Schematic of the Brayton Cycle

A temperature versus entropy (T-S) plot for the ideal Brayton cycle can be found in Figure 3. The cycle begins with the working fluid entering the inlet of the compressor, depicted in Figure 2 and Figure 3, as state point 1, where it is pressurized and consequently heated via the pressurization process. This process, shown by the jump in pressure lines from point 1 to point 2 on the T-S plot in Figure 3, increases the density, pressure, and temperature of the air. The ratio of the pressure 'after' to 'before' the compressor is known as the pressure ratio. The exit of the compressor is state point 2. The working fluid then flows to a heat exchanger where the working fluid is heated at constant pressure, increasing its energy content. This heating process models the burning of fuel in the combustion chamber and is shown by the process from state point 2 to

state point 3, the exit of the heat exchanger. The working fluid then expands through the gas generator turbine, converting energy to rotational kinetic energy of the spinning gas generator turbine shaft. The expansion process, shown on the T-S plot as the path from state point 3 to state point 4, the gas generator turbine exit, causes a decrease in the temperature and pressure of the working fluid. Since the gas generator turbine is mechanically linked to the compressor by a shaft, as shown in Figure 2, this power is utilized to run the engine's compressor and auxiliary systems, such as oil pumps and fuel pumps. The working fluid then expands through the power turbine whose output shaft is connected to a gearbox where the power is used to propel aircraft, helicopters or ships or produce electricity by driving an electric generator. As with the gas generator turbine, the conversion of energy to work results in a decrease in temperature and pressure of the working fluid at the power turbine exhaust. This can be seen as the process path from state point 4 to state point 5, the power turbine exhaust, on the T-S plot. In the operation of a real gas turbine engine, the working fluid then exhausts from the engine to the local ambient pressure; however in the Brayton cycle, the working fluid returns to state point 1 through a heat exchanger which carries out a constant pressure heat rejection process. Even though the working fluid is at a higher temperature at state point 5 than it was at state point 1, it can do no further expansion work as it is no longer at increased pressure. From state point 5, the ambient cools the working fluid isobarically, and thus returns the working fluid to state point 1, completing the cycle.

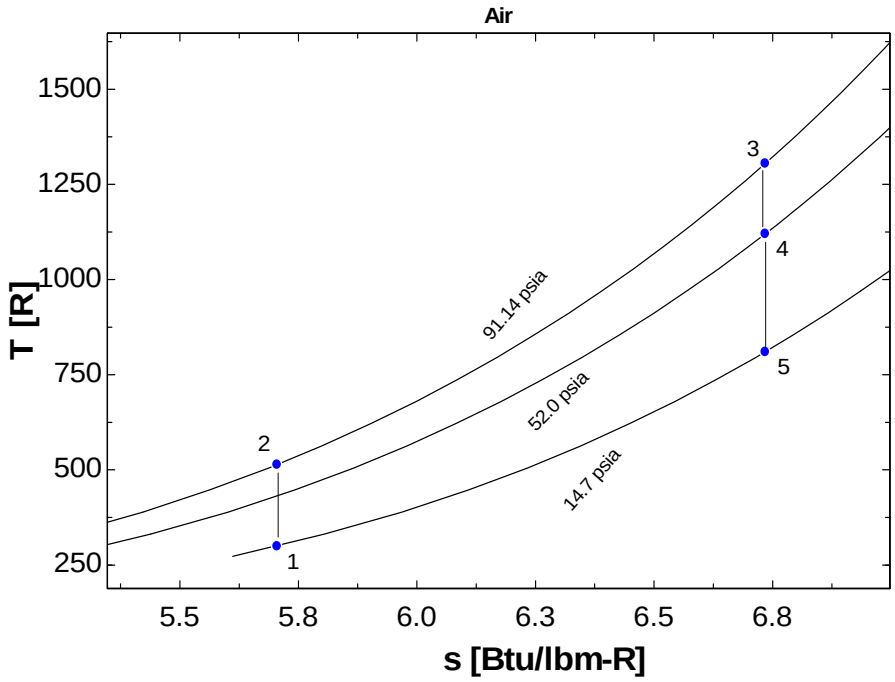

Figure 3 Temperature vs Entropy Plot for Turboshaft Brayton Cycle

Much of the power generated from the expansion of the working fluid through the turbines is consumed by the compressor and the auxiliary systems. As long as gas turbine engines have been in use, there has been constant effort to increase the amount of power that can be generated. One way to do this is to decrease the compressor's power consumption while still attaining the same pressure ratio. If this could be accomplished, more power would be available for the power turbine and would ultimately be sent to the output shaft.

One way to decrease the work of the compressor, while still maintaining the same pressurization, is to decrease the specific volume of the air as it is being compressed. The work of compression for a steady flow process is given by Equation 1, where w is the work per unit mass of compression, v is the specific volume of the working fluid, which is the volume per unit mass, and dP is the differential change in pressure.

$$w_{compression} = -\int v dP \qquad \text{Equation 1}$$

From reorganization of the ideal gas law, shown in Equation 2, specific volume is dependent on temperature, *T*, pressure, *P*, and the gas constant, *R*. It can be seen that specific volume is proportional to temperature.

$$v = \frac{RT}{P} \qquad \text{Equation 2}$$

Figure 4 is a pressure versus specific volume (P-ν) plot for a typical pressurization process. According to Equation 1, work for a steady flow process is the integral of specific volume with respect to pressure, which is represented on a P-ν plot as the area to the left of a process curve. The compression process for the ideal Brayton cycle is isentropic, which would follow the line of constant entropy, shown in Figure 4. If pressurization could be carried out isothermally, this process would follow the line of constant temperature in Figure 4. Figure 4 illustrates that there is less area to the left for the isothermal process path than for the isentropic process path, meaning an isothermal pressurization process requires less work, and thereby power, than an isentropic one. Isothermal pressurization is achieved in a gas turbine engine by cooling the working fluid as it is pressurized. Water Fog Injection (WFI) is a method that results in cooling across the compressor, which approaches the effects of isothermal pressurization.

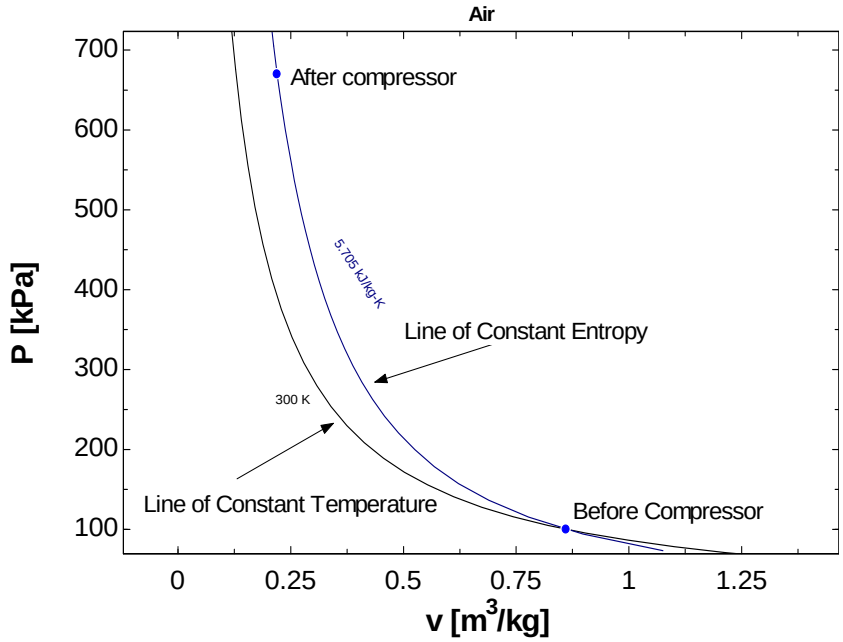

Figure 4 Pressure vs Specific Volume Plot for a Typical Pressurization Process

Urbach investigated Water Fog Injection into the compressor inlet of larger gas turbines in an attempt to reduce the nitrous oxide (NO_x) emissions from marine power plants [1]. Experiments using the LM2500 revealed that water fog injection caused a reduction in the concentration of NO_x and an increase in net power. Water has a higher heat capacity than air, and therefore its presence in high temperature environments tends to have a cooling effect on air. The water's cooling effect in the compressor caused the increased net power, while the lower temperatures in the combustor decreased the NO_x levels [1].

According to Chaker, Meher-Homji, and Mee, research has been conducted on gas turbine inlet fogging, but it has focused on gas turbines ranging from 5 to 250 MW (6700 to 335,000 horse power) [2]. There appears to be little research concerning WFI for smaller engines. This is troubling for two reasons. First, this leaves out a large range of gas turbine engines that are employed in numerous applications. Secondly, and perhaps more importantly, there are distinct differences between larger gas turbine engines, with higher pressure ratios, and

small gas turbines, with much lower pressure ratios. A lack of investigation in WFI in small engines represents an interesting frontier in application and innovation. This research project challenged that frontier through an experimental investigation of water fog injection into the compressor inlet of a Rolls-Royce Model 250-C20B gas turbine, a representative small gas turbine engine.

Two Rolls-Royce Model 250-C20B gas turbines were recently acquired by the US Naval Academy. The Model 250-C20B is comprised of a six stage axial compressor, a single stage centrifugal compressor, a single combustion chamber, a two stage gas generator turbine, and a two stage power turbine, all of which are shown in Figure 5.

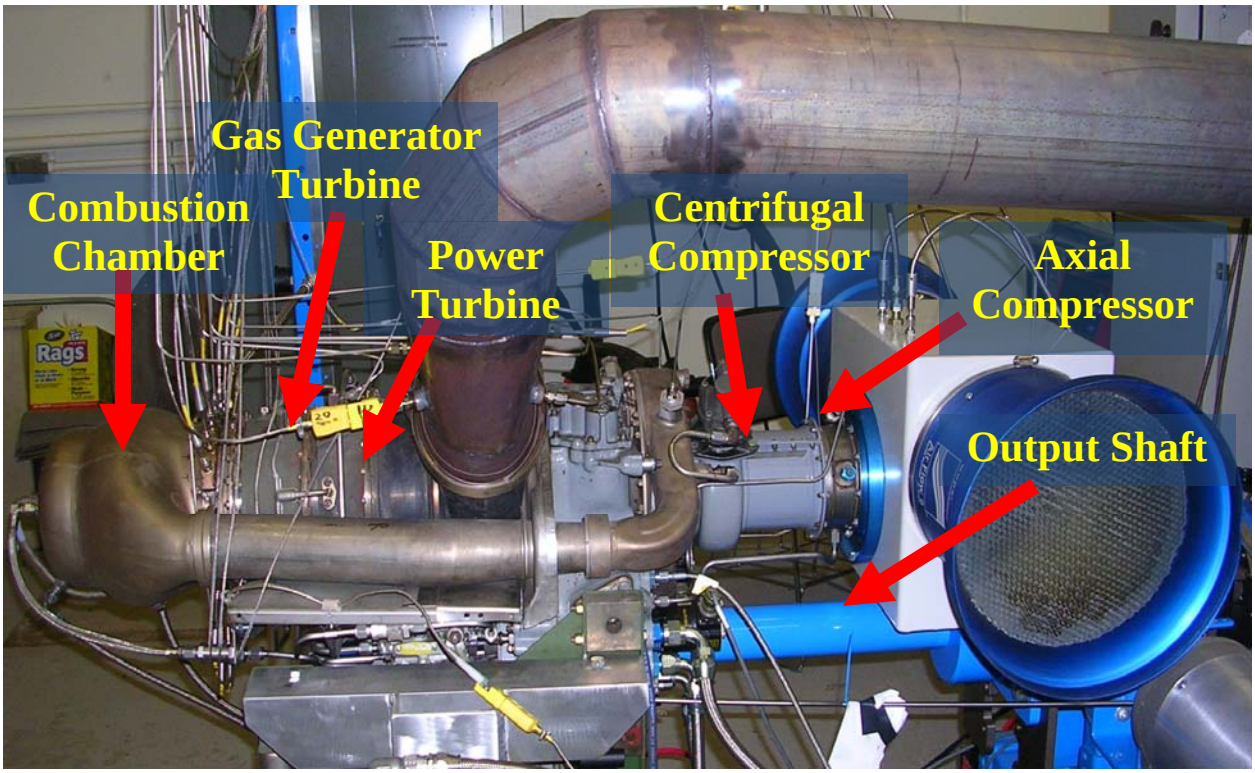

Figure 5 The Model 250-C20B

The Model 250 class of engines is widely used by the military. The Model 250-C20B is a predecessor of the engines currently employed by the U.S. Army in the OH-58 “Kiowa

Warrior" and the AH-6 "Little Bird," which are shown in Figure 6. The Navy also employs a version of the Model 250 in its RQ-8 "Fire Scout" Vertical Takeoff Unmanned Aerial Vehicle (VTUAV), the Model 250-C30R/3. In addition to wide military use, the Model 250 family is also very popular in the civilian sector. According to Rolls Royce, every major helicopter manufacturer has an aircraft which uses a member of the Model 250 family [3].

Figure 6 The AH-6 and the OH-58, which use versions on the Model 250

To illustrate the differences between the Model 250-C20B and larger, higher pressure ratio engines, contrast it with the LM2500. Table 1 gives important characteristics of each engine. The LM2500 weighs over 75 times as much as the Model 250-C20B and produces 80 times more power. As can be seen, there are considerable differences between one of the most common larger gas turbines and the Model 250-C20B.

	LM2500	Model 250 C-20B
Weight	10,300 lb	136 lb
Max Power	33,600 shp	420 shp
# of Stages in Compressor	16	7
Pressure Ratio	18:1	7:1

Table 1 Significant Characteristics of the Model 250 and the LM2500 [4], [5]

The most significant difference between the smaller Model 250-C20B and larger gas turbine engines when considering water fog injection is the difference in pressure ratios. As

stated, the goal of WFI is to achieve a cooling effect on the air in the compressor. This cooling effect is achieved through heat transfer from the air to the water fog in both sensible and latent forms. The sensible heat transfer is associated with the change in temperature of the liquid water and the latent heat transfer with the production of water vapor. This capability for heat transfer, and cooling, is directly related to the pressure ratio of the engine.

The effect of varying pressure ratios on possible heat transfer to water fog depends upon the fact that different pressure ratios create different changes in temperature across a compressor. This relationship is modeled by Equation 3, which shows how the temperature ratio and pressure ratio are related for an isentropic process. In this equation 'k' is the specific heat ratio for a given fluid. As pressure ratio increases, temperature ratio increases. A larger pressure ratio equates to a larger temperature ratio.

$$\frac{T_2}{T_1} = \left(\frac{P_2}{P_1} \right)^{k-1/\ k} \qquad \text{Equation 3}$$

Another way to represent the pressurization processes of the LM2500 and the Model 250-C20B is on a T-S plot. Figure 7 is a T-S plot of the thermodynamic compression processes with no water injection for the LM2500 and the Model 250-C20B. For the sake of comparison it assumes an isentropic efficiency of 90% for each engine.

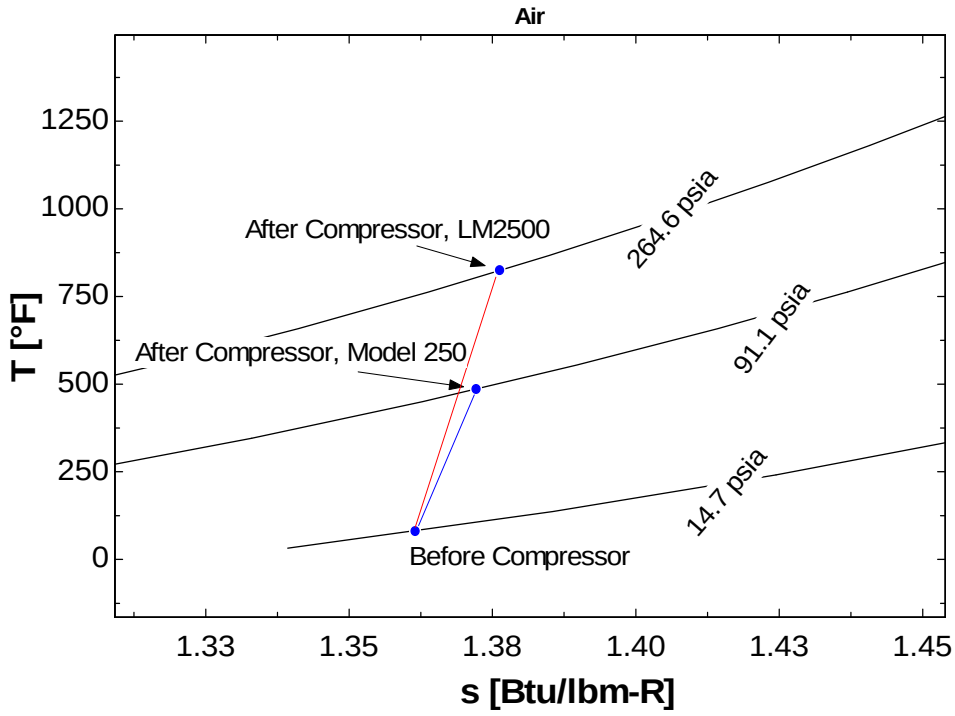

Figure 7 A Temperature vs. Entropy Plot for the Compression Process

The compression process for the LM 2500 is shown by the red line and represents the maximum pressure ratio of 18:1. The blue line represents the compression process for the Model 250-C20B and represents a maximum pressure ratio of 7:1. The curved lines are isobars, meaning lines of constant pressure. Figure 7 shows the temperature difference is greater in for the LM2500 than it is for the Model 250. The larger temperature difference constitutes a larger thermal potential which would lead to a higher rate of heat transfer from air to water when there is water fog injection. The smaller difference in temperature from the lower pressure ratio could mean that water fog injected into the Model 250-C20B wouldn't experience the same heat transfer from air to water, and thus wouldn't experience the same level of cooling across the compressor. If this were the case, the water might not reach saturation conditions in the compressor, meaning it would not evaporate, causing liquid water to propagate through the compressor and into the combustor. This investigation determined the effects of the uncertainty

of whether water fog injection holds the same benefits for a large and small engine such as the Model 250-C20B.

II. Theory

Many different metrics are used to characterize the operation of a gas turbine engine. These metrics are capable of being calculated if one knows the temperature and pressure of the working fluid at various state points, the mass flow rate of the operating fluid and the mass flow rate of the fuel. If the speed and torque of an output shaft and emissions data are also available, one can quantify the efficiency, the powerfulness, and the environmental impact of any gas turbine engine.

Engine analysis starts by following the sequence of thermodynamic state points beginning with the compressor inlet. The isentropic efficiency of the compressor describes how much energy the actual compressor consumes compared to an ideal, isentropic compressor. The ideal compressor specific work is determined by taking the measured compressor inlet temperature and pressure and the actual pressure ratio and calculating what the temperature would be for the compressor discharge for an isentropic process. This is compared to the actual temperature through the use of enthalpies, which are dependent upon only the temperature of the working fluid. A subscript of "s" indicates that the value is an isentropic value, meaning that it is what would result if the process to reach that state point had been carried out isentropically. A subscript of "actual" indicates that this value was determined from measured data. The comparison of compressor isentropic efficiency is given by Equation 4.

$$\eta_c = \frac{w_{isentropic}}{w_{actual}} = \frac{\left(h_{2,s} - h_1\right)}{\left(h_{2,actual} - h_1\right)} \qquad \text{Equation 4}$$

The heat input to the Model 250-C20B represents the energy that the engine consumes to provide useful power. The heat input can be determined by two methods. The first method is to

use the mass flow rate of the fuel and the lower heating value of the fuel (LHV), and is shown in Equation 5. This represents the ideal heat input to the engine.

$$\dot{Q}_{in,ideal} = \dot{m}_{fuel} LHV_{fuel} \qquad \text{Equation 5}$$

The actual heat input to the working fluid is calculated from an energy balance using enthalpies and is shown by Equation 6. The enthalpy for state point 3 is dependent on the measured combustor temperature, while the enthalpy of state point 2 is dependent on the measured compressor discharge temperature.

$$\dot{Q}_{in} \approx \left(\dot{m}_{air} + \dot{m}_{fuel}\right) h_3 - \dot{m}_{air} h_2 \qquad \text{Equation 6}$$

The ratio of the actual heat input to the ideal heat input is known as the combustion efficiency, η_b. This relationship is shown as Equation 7.

$$\eta_b = \frac{\dot{Q}_{in,actual}}{\dot{Q}_{in,ideal}} \qquad \text{Equation 7}$$

The gas generator turbine powers the compressor and the auxiliary systems of the Model 250-C20B. Its power is given by Equation 8. The enthalpy at state point 4 is determined based on the measured temperature at the discharge of the gas generator turbine. The measured mass flow rates of fuel and air are also needed to calculate the power of the GGT.

$$\dot{W}_{GGT} = \left(\dot{m}_{air} + \dot{m}_{fuel}\right)\left(h_3 - h_4\right) \qquad \text{Equation 8}$$

The isentropic efficiency of the gas generator turbine is calculated in a manner similar to the isentropic efficiency of the compressor. The efficiency is determined based on the measured temperatures and pressures before and after the gas generator turbine and what the temperature would be for an isentropic expansion process. The isentropic efficiency of the GGT is given by Equation 9.

$$\eta_{ggt} = \frac{w_{actual}}{w_{isentropic}} = \frac{\left(h_3 - h_{4,actual}\right)}{\left(h_3 - h_{4,isentropic}\right)} \qquad \text{Equation 9}$$

The power of the power turbine represents the useful power of the engine. The power of the power turbine is based upon the mass flow rates of the air and fuel, and the enthalpies of its inlet and outlet. The enthalpies at the power turbine inlet and the exhaust are determined from the temperatures measured at those points. The power of the power turbine is given by Equation 10.

$$\dot{W}_{PT} = \left(\dot{m}_{air} + \dot{m}_{fuel}\right)\left(h_4 - h_5\right) \qquad \text{Equation 10}$$

The isentropic efficiency of the power turbine is calculated exactly the same as the isentropic efficiency of the gas generator turbine, except using the measured temperatures and pressures and the calculated isentropic temperature for state points 4 and 5, the Gas Generator Turbine discharge and the Power Turbine discharge, respectively. The isentropic efficiency is given by Equation 11.

$$\eta_{pt} = \frac{w_{actual}}{w_{isentropic}} = \frac{\left(h_4 - h_{5,actual}\right)}{\left(h_4 - h_{5,isentropic}\right)} \qquad \text{Equation 11}$$

The calculated power of the power turbine is the net power of the engine before it passes through the reduction gear box. There are inefficiencies associated with the reduction gears, so there is a difference in the net power as calculated by the thermodynamic model and the actual power measured by the dynamometer. The ratio of the actual power to the thermodynamic power is the mechanical efficiency.

The brake specific fuel consumption (BSFC) is the ratio of the mass flow rate of fuel consumed to the shaft horse power (SHP). A smaller BSFC means that larger amounts of the chemical energy of the fuel are being converted to useful work. It is given by Equation 12.

$$BSFC = \frac{\dot{m}_f}{SHP} \qquad \text{Equation 12}$$

The thermal efficiency represents the ratio of the useful power achieved to the thermal power consumed in the process. It is given by Equation 13.

$$\eta_{th} = \frac{\dot{W}_{net}}{\dot{Q}_{in}} \qquad \text{Equation 13}$$

It can also be calculated based upon the measured shaft power and the measured mass flow rate of fuel. This metric would better be referred to as whole engine efficiency, as it would take into account the mechanical inefficiencies of the reduction gear box in addition to the thermodynamic inefficiencies. It is given by Equation 14.

$$\eta_{th} = \frac{SHP}{\dot{m}_{fuel} LHV_{fuel}} \qquad \text{Equation 14}$$

III. Experimental Setup

The objective of this investigation was to determine the effect of water fog injection on the Model 250-C20B. The effect was investigated by following a test matrix that varied engine throttle setting and the mass flow rate of water injected into the gas turbine engine. Water fog was injected into the air stream immediately upstream of the gas turbine's compressor inlet by a developed spray system. The effect of the water fog injection on the engine was observed using several parameters including net power, engine thermal efficiency, component efficiencies for the compressor and each turbine, Brake Specific Fuel Consumption, and exhaust gas composition. These metrics were calculated for each test point based on data acquired through the engine data acquisition system. Comparisons were made at different water mass flow rates and engine power settings.

A. Instrumentation

In order to calculate the different metrics used to characterize the effect of water injection on the operation of the Model 250-C20B, high quality data were acquired. The Model 250-C20B is an operational engine, and as such was never originally intended to be used for research purposes. In order to collect the necessary data, instrumentation was retrofitted to the engine. This work was carried out by laboratory technicians of the United States Naval Academy Engineering and Weapons Division Technical Services Department over the summer of 2007 and the beginning of the fall 2007 academic semester. The pressure transducers were calibrated to ensure accuracy. The calibration file provides the slope and y-axis intercept of the system's linear calibration and is included as Appendix A.

The temperatures and pressures at the key thermodynamic state points of the engine were collected. These state points are illustrated in Figure 8 and Table 2. They match with the state points described in Figure 1 and Figure 2.

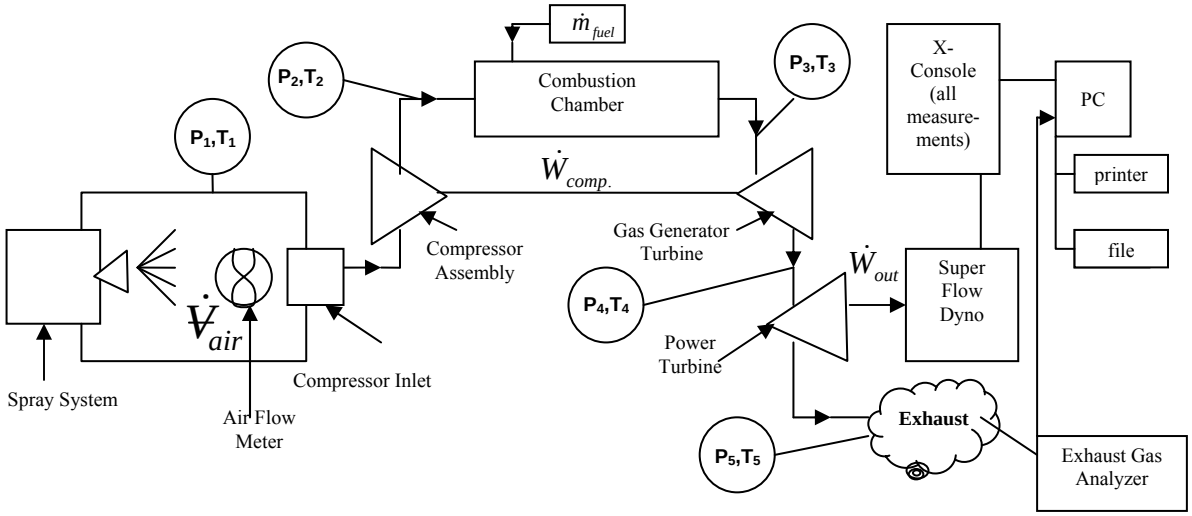

Figure 8 A Schematic Representation of the Experimental Setup

State Point	Engine Location
1	Compressor Inlet
2	Compressor Discharge/ Combustor Inlet
3	Combustor Discharge/ Gas Generator Turbine Inlet
4	Gas Generator Turbine Discharge/ Power Turbine Inlet
5	Power Turbine Discharge

Table 2 State Point List

With the exception of the Kiel Probes at the compressor discharge, all of the pressure probes in the data acquisition system measure static pressure. While static pressure was mostly used in the thermodynamic analysis of the tests, the total pressure was needed to determine the total pressure ratios, a common performance metric in internal flows. The total temperature was determined by the addition of the flow specific kinetic energy to the temperature through

Equation 15. In this equation T is the local temperature, T_o is the total temperature, V is the magnitude of the velocity and c_p is the constant pressure specific heat of the fluid. The process by which a flow is brought to rest to determine total properties is assumed to be isentropic. Therefore, the isentropic relationship given in Equation 16 was used to calculate total pressure from the static pressure, the static temperature and the total temperature.

$$T_0 = T + \frac{V^2}{2c_p} \qquad \text{Equation 15}$$

$$\frac{T_o}{T} = \left(\frac{P_o}{P}\right)^{k-1/\ k} \qquad \text{Equation 16}$$

The temperature at each state point was known from the collected data. The specific heat at constant pressure was determined for the given temperature and pressure at the state point. The velocity at each state point was determined by use of the conservation of mass principle given in Equation 17.

$$\dot{m} = \rho A v_{avg} \qquad \text{Equation 17}$$

The mass flow rate of air through the engine was known from the collected inlet air data. The density was calculated based upon the measured temperature and pressure at each state point. This left the area and average velocity as the only unknowns. The cross sectional flow area for each state point was measured on a Model 250 display that the Academy owns. These areas were then used to estimate the average velocity needed to calculate the total temperature, which was needed to calculate the total pressure.

State point 1 is the compressor inlet and is located inside the housing known as the air box. At this point two thermocouples measured the temperature of the air, while one pressure probe measured the static pressure. The configuration is shown in Figure 9.

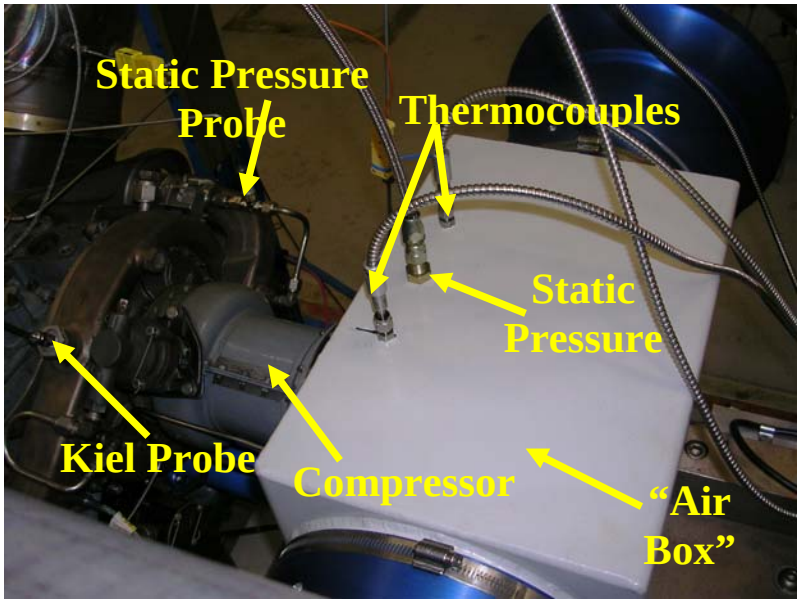

Figure 9 Air Box and Compressor Inlet

The temperature and pressure at the compressor discharge, state 2, were measured in the air scrolls on both sides of the engine by sensors that combine a Kiel probe and a thermocouple. A Kiel probe is a total pressure probe that is resistant to variations in flow angle. These sensors are also shown in Figure 9. In order to convert this static pressure to total, the area of the air scrolls was measured on a display model of the Model 250. Based on the volumetric air flow and the measured area, an estimated average air velocity at the compressor discharge was obtained as shown in Equation 17. This conversion can be found as part of the analysis code in Appendix B the EES code. The exit of the combustion chamber is the third thermodynamic state point. Temperature and pressure measurements were made by a sensor ring of fourteen

thermocouples and two static pressure probes arranged around the circumference of the combustor as seen in Figure 10.

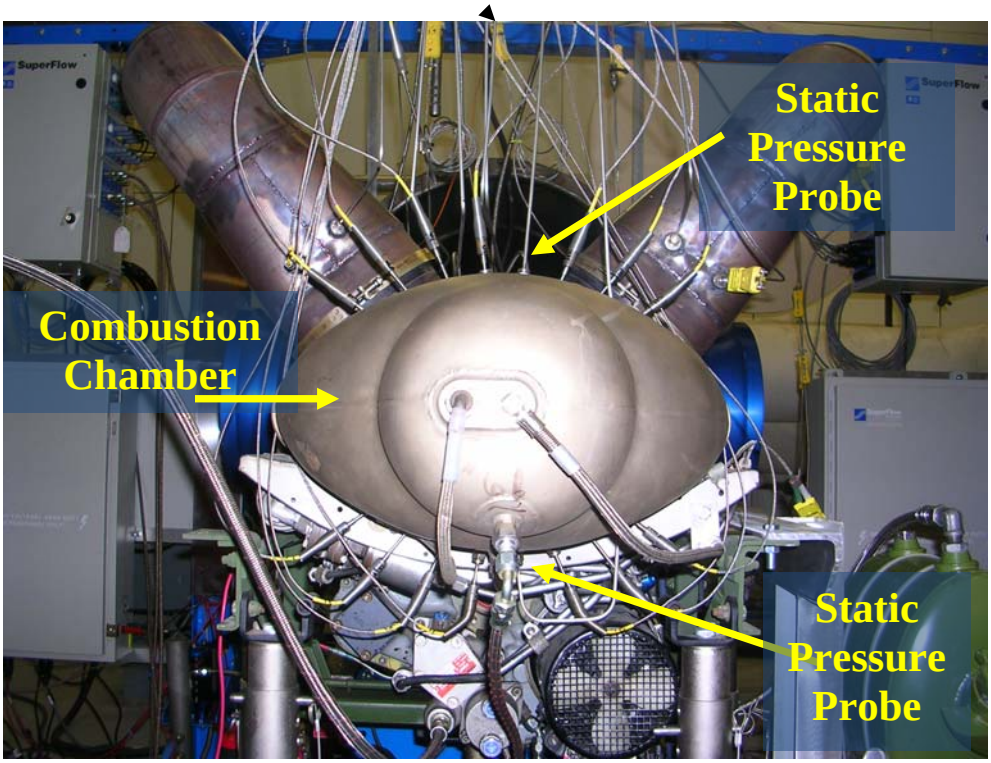

Figure 10 Combustion Chamber with Sensor Ring

The fourteen thermocouples, as shown in Figure 11, were arranged such that four were at depth "A" of 3 inches, six were at depth "B" of 3.125 inches, and six were at depth "C" of 3.75 inches. Different sampling depths were used in order to acquire the most representative measurement of the average combustor temperature. The static pressure probes were at a depth of 3.5 inches. The flow area of the combustion chamber at the location of the probes was measured on the display model of the Model 250 in order to convert the static pressures to total pressures. This conversion process is also found in Appendix B.

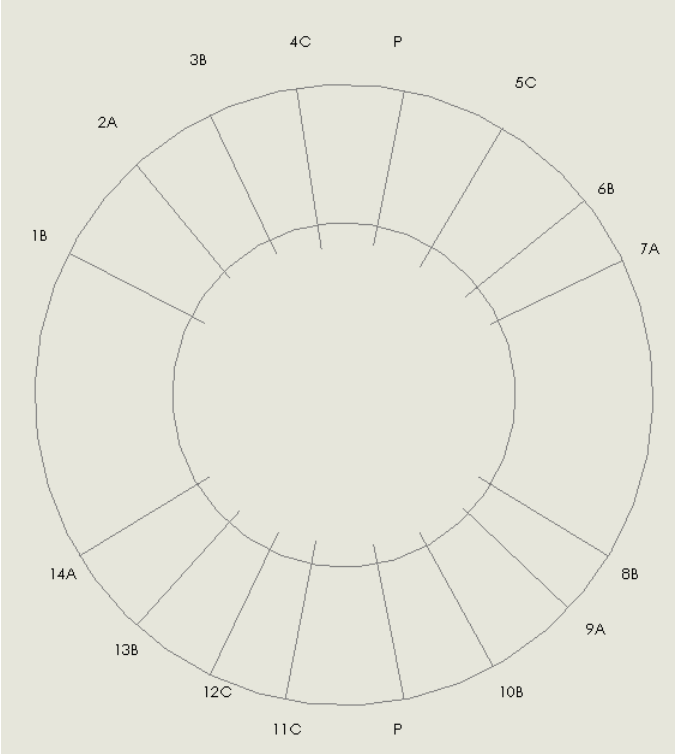

Depth A=3 in
Depth B=3.125 in
Depth C=3.75 in

Figure 11 Combustion Chamber Sensor Ring Drawing

The temperature after the gas generator turbine and before the power turbine, state point 4, was measured by a harness of 4 thermocouples shown in Figure 12. These thermocouples were original manufacturer equipment and were designed to be automatically averaged. When the engine is installed onboard an aircraft this average gas generator turbine discharge temperature is monitored by the pilot in the cockpit. One of the thermocouple mountings was modified by lab technicians to accept a static pressure probe, as illustrated in Figure 12. A measurement of the flow area at the gas generator turbine on the display model was used to convert the measured static pressure to total pressure as described in Appendix B.

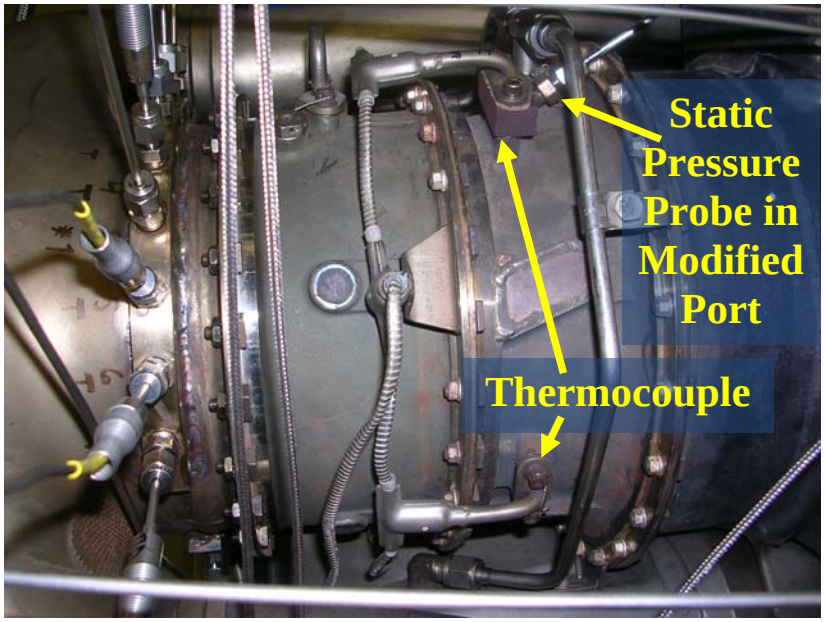

Figure 12 Gas Generator Turbine Exit Sensor Harness

The pressure of the exhaust of the power turbine, state point 5, was measure by four static pressure probes, two mounted in each exhaust stack. The temperature downstream of the power turbine was measured in four locations: two thermocouples were located in the body of the engine directly behind the power turbine; two others were located in the exhaust stacks, one in the left, and one in the right. As with the other state points, measurements of the flow area after the power turbine from the display model were used to convert the static pressures to total pressure. This conversion was based upon Equation 15, Equation 16 and Equation 17 and can be found in Appendix B.

Other data important to the analysis of the engine's operation were also collected. The volumetric flow rate of the air entering the compressor inlet was measured by two turbine flow meters mounted on either side of the air box and can be seen in Figure 13. The volumetric flow rate of the air was used to calculate the mass flow rate of air into the engine, which was used extensively in the thermodynamic analysis. The mass flow rate of fuel was measured by a

turbine wheel flow meter in the fuel line and was used in the calculation of the Brake Specific Fuel Consumption. The torque and the speed of the output shaft were measured and resisted by the SuperFlow™ dynamometer which can be seen in Figure 13. The speed of the gas generator turbine and the power turbine were also measured via tachometers and fed to the SuperFlow™ dynamometer box.

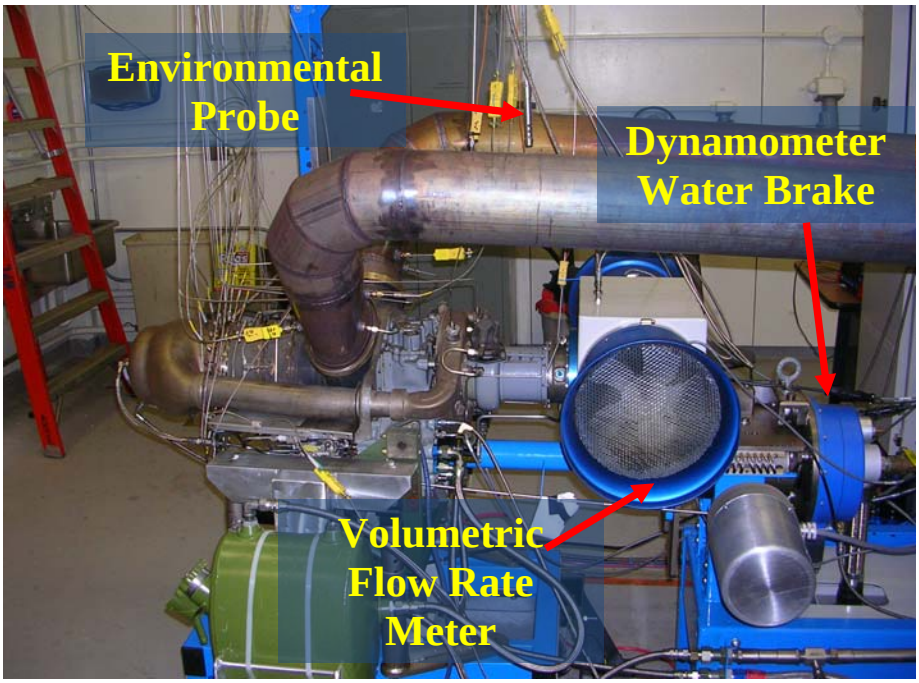

Figure 13 Other Instrumentation

Exhaust gas composition was measured by an Infrared Industries, Inc. five gas analyzer from a probe in the left exhaust stack, and is shown in Figure 14. This gave the concentration, in parts per million, of unburned hydrocarbons, nitrous oxides, and the percentage of carbon monoxide, carbon dioxide, and oxygen. The vapor pressure, local barometric pressure and the local test cell air temperature were measured by an environmental probe, shown in Figure 13. The dynamometer system used this data to calculate relative humidity and air density.

Figure 14 Exhaust Gas Analyzer and its Probe

B. Spray System

To meet the objective of determining the thermodynamic effects of water fog injection on the Model 250, a spray system was developed to meet two thermodynamically significant requirements: mass flow rate of water and spray droplet size.

The first requirement of the spray system was precise delivery of desired water mass flow rate. The spray system must be precise enough to deliver variable mass flow rates reliably from low to high based on the percentage of the engine total mass flow. Spraying too much water could cause the temperature in the combustion chamber to drop to such an extent that the engine can no longer sustain operation. This is a situation to be avoided as the sudden stalling of the engine could cause damage to the engine and could potentially have catastrophic consequences. For this reason, the maximum volumetric flow rate of water has been set to 1.6 gallons per minute, which is approximately 6% of the maximum mass flow rate of air through the engine for the normal operation.

The second requirement that the spray system met was the droplet size of the fog. The objective of this investigation was to determine the thermodynamic effects of water fog injection on the Model 250-C20B, so it was desired that the fog actually have a cooling effect in the compressor. For this to be possible, the heat transfer from the air in the compressor to the water

fog had to be maximized. The controlling factors of the rate of heat transfer are temperature difference and surface area. The temperature difference was set by the compressor performance and the initial water temperature, which was approximately room temperature. The surface area for the heat transfer between the air and the water was controlled via droplet size. A larger surface area for a given volume of water requires a larger number of small droplets. Therefore, the spray system was designed with the objective of minimizing the spray droplet size. Urbach claimed the ideal droplet size had a diameter of 10μm; however, due to cost concerns and a desired simplicity of design, the goal for this spray system was a 50μm diameter droplet [1].

The spray system was designed to produce the water fog as water was forced through spray nozzles by hydraulic pressure. A basic schematic for the spray system design is shown in Figure 15.

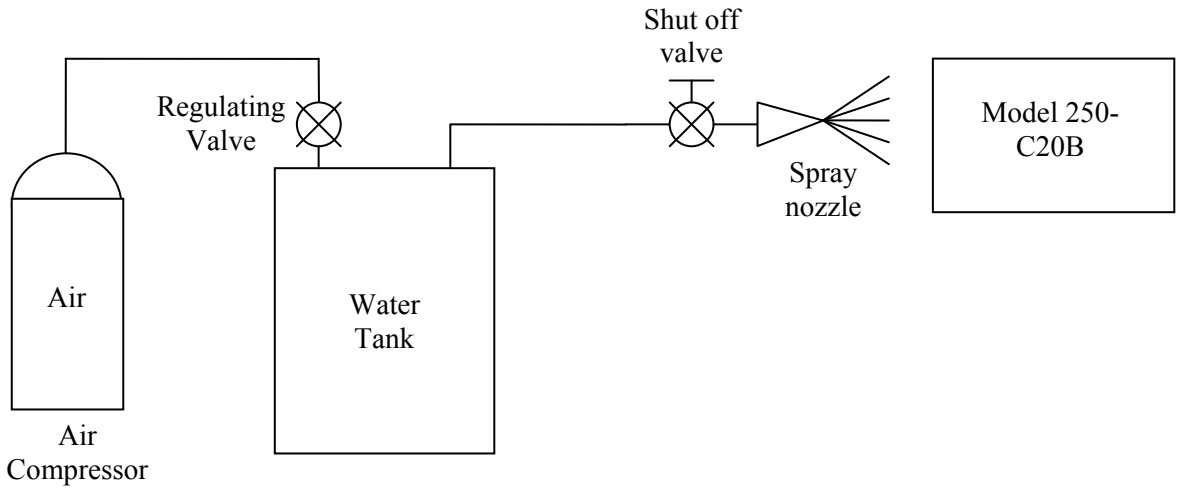

Figure 15 Schematic Representation of the Spray System

The system consists of a 30 gallon water tank that supplied approximately 20 minutes of spray time at maximum volumetric flow rate. The water tank was pressurized by compressed air from a shop air compressor. The pressure applied to the tank was controlled by a regulating valve.

An electrically controlled solenoid valve operated from the engine control room was used to initiate the water spray after the engine had been started and reached acceptable operating conditions. The water was forced through the spray nozzle to produce the desired fogging effect. The spray system is shown as Figure 16.

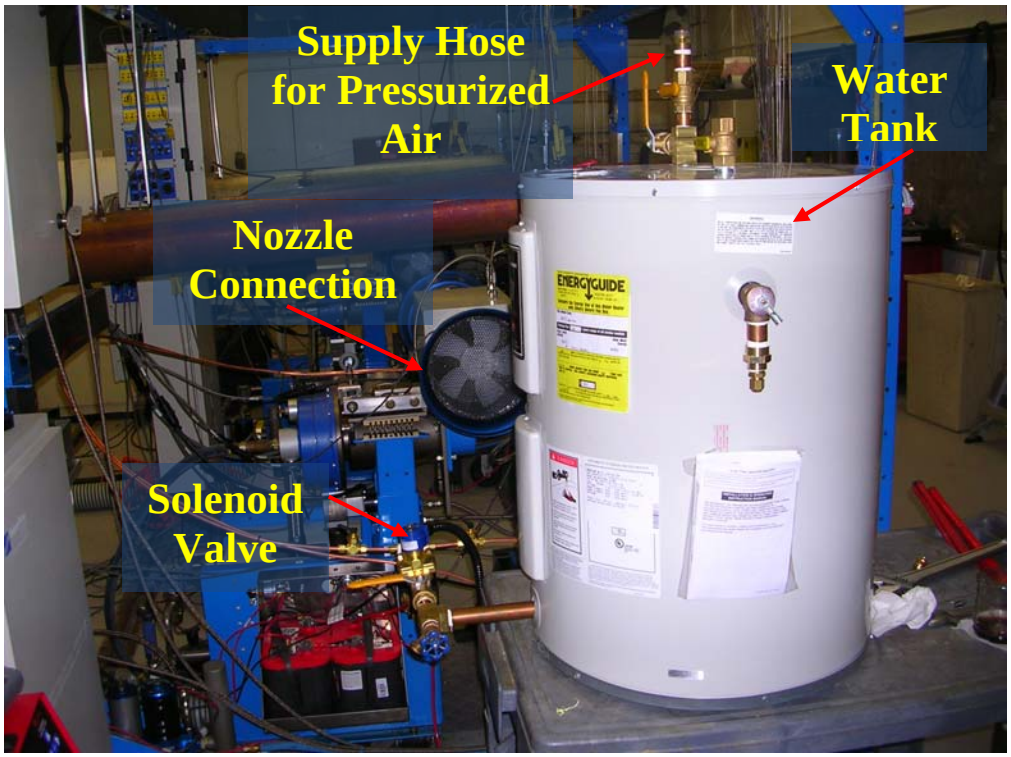

Figure 16 Preliminary Spray System

Two spray nozzles were investigated and used in the operation of the spray system: the ¼ LNN-10 and the ¼ LNN-26 from Spraying Systems Company, which are shown in Figure 17.

Figure 17 Selected Spray Nozzles

These nozzles were selected based upon their ability to deliver the required volumetric flow rates and the desired spray droplet sizes at reasonable hydraulic pressures. Table 3 shows measured back pressures required to achieve desired water flow rates. These nozzles were also selected based on the manufacturer's statement that each was capable of delivering a majority of droplets with diameters smaller than 50 μm.

Volumetric Flow Rate	0.8 gpm	0.4 gpm	0.2 gpm
¼ LNN-10	920 psi	236 psi	58.6 psi
¼ LNN-26	137 psi	33.7 psi	7.66 psi

Table 3 Required Hydraulic Pressure to Achieve a Given Flow Rate

The volumetric flow rate of the spray system was varied by changing the back pressure of the water. This was achieved by regulating the air pressure that was applied to the water tank. The water flow rate was also altered by exchanging nozzles of different capacities. Spray nozzles produce smaller droplets at higher pressures; therefore, the combination of nozzles that allowed operation at the highest pressures available was chosen. Though the sizes of individual droplets

were never measured, it was assumed that using the highest possible pressure would cause the droplet sizes to match the manufacturer's data.

The spray nozzles were mounted in the air box in front of the compressor inlet. They were mounted such that all of the spray entered the compressor inlet at every conceivable back pressure. The nozzle installation can be seen in Figure 18.

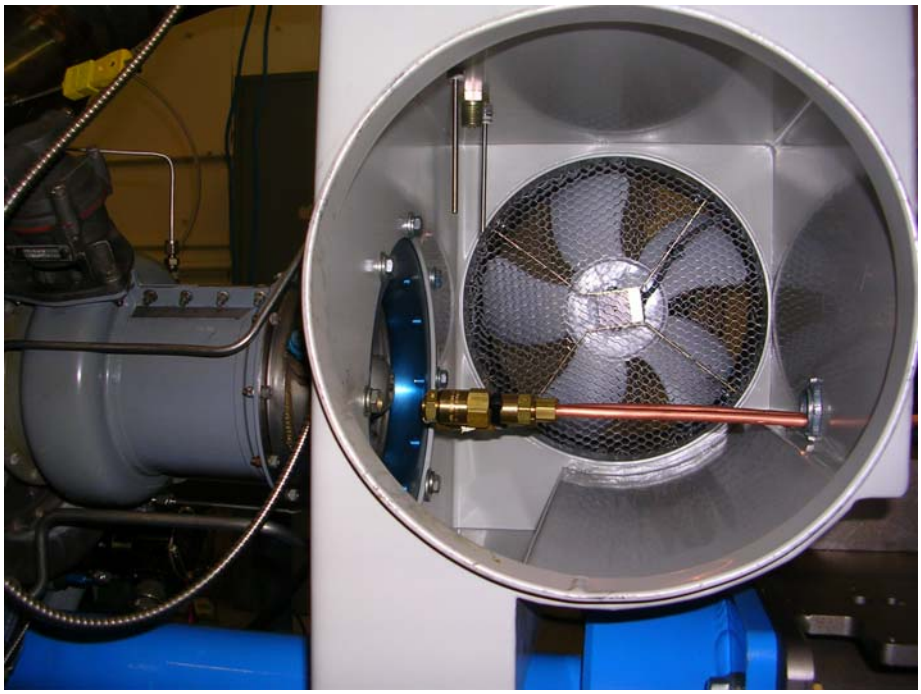

Figure 18 Image of Spray nozzle installation

C. Data Acquisition and Procedure

Operation of the Model 250-C20B was governed by standard procedures, which are included as Appendix C. Tests were carried out for ten water flow rates: 0 gallons per minute (gpm) also known as the "No Spray" test, 0.1 gpm, 0.2 gpm, 0.3 gpm, 0.5 gpm, 0.7 gpm, 0.8 gpm, 1.0 gpm, 1.2 gpm, and 1.4 gpm. These tests were carried out with an output shaft speed of 6016 rpm as this was the design speed for the engine in application. Two parameters were

varied: engine throttle setting and water volumetric flow rate. For the operation of the engine, the throttle setting as a percentage ranged from 30% to 100%.

A standard test of the engine began by idling the engine at the 30% throttle setting. From 30% throttle to 65% throttle the output shaft speed is still changing. At 65% the output shaft speed is 6016 rpm, the design point. This speed was restricted by the dynamometer in order to operate the engine as it would have been operated in application. From 65% to approximately 72% the bleed air valve that is located between the 6^{th} centrifugal stage of the axial compressor and the centrifugal compressor is open. This is part of the engine's normal start up operation. When the bleed air valve is open, not all of the air that enters the compressor inlet proceeds all the way through the engine. The bleed air valve is closed from 72% to 100 % throttle. According to the Model 250 operation and maintenance manual, 100% throttle, which would be 420 shaft horse power, was only utilized for take offs and emergency situations. The cruise power of the engine was 375 shp. The throttle percentage that was required to achieve this power varied with the water spray flow rate, but for the normal operation of the engine it was approximately 90% throttle. Through the course of a test, the throttle percentage was adjusted by 1 % increments. For each test, the engine throttle was increased from 30% to 100% and then was deceased back down to 30%. Data were measured at increments of 5% from 30% to 65% and increments of 1% from 66% to 100%.

For each throttle percentage setting the corrected mass flow rate of air was calculated. This was done so that comparisons of effects on the engine could be made against an accepted metric. These calculations were carried out in the data reduction program. The coding for this program can be found in Appendix B. One of the effects of WFI on the engine was that the mass flow rate of air increased for a specified percent throttle for the 0.1 gpm and 0.2 gpm tests but

decreased for flow rates larger than 0.3 gpm water spray flow rate test. This relationship is shown in Figure 19, a graph of average corrected mass flow rate of air vs. throttle setting.

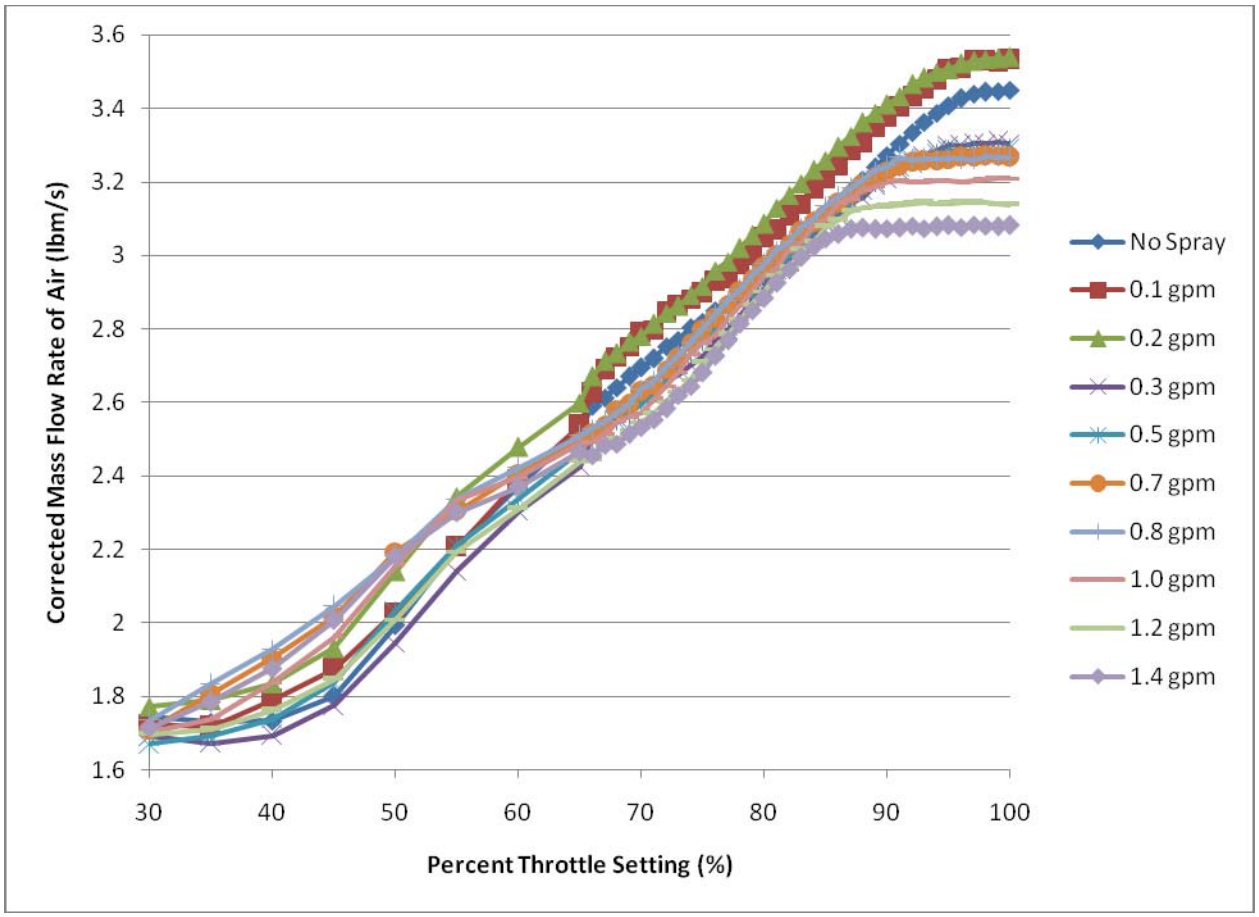

Figure 19 Corrected Mass Flow Rate of Air vs. Throttle Setting

For ease of comparison, Table 4 shows the relationship between percent throttle setting, corrected mass flow rate of air, and engine net power corrected for standard temperature and pressure (STP Power) at significant points in a typical no spray test.

Percent Throttle (%)	Corrected Mass Flow Rate of Air (lbm/s)	STP Power (Corrected hp)	Test Point Activity
65	2.52	99.5	Spray Initiation/ engine reaches speed
72	2.64	164	Bleed Air Valve Closed
90	3.15	355	Approx. Cruise Power
100	3.31	418	Max Power

Table 4 Test Event Comparison

As mentioned, the volumetric flow rate of water was varied from 0 gpm to 1.4 gpm. Multiple tests were conducted for each water flow rate. As was mentioned in Table 4 , water spray was initiated at 65% throttle setting through the activation of the solenoid valve. This throttle setting was chosen because it was when the output shaft speed reached the design speed of 6000 rpm. Water spray occurred as the throttle increased up to 100% and as it decreased back down to 65%. Water spray was also terminated at 65% when shutting the engine down. Enough time was allowed for the engine to dry itself out before it was shut down. When multiple tests occurred on a single day, the water tank level was topped off between tests to ensure that conditions were identical between tests.

D. Data Reduction and Computer Models

Data reduction was performed to determine the effects of WFI on the Model 250-C20B. The data reduction used multiple programs including WinDyn, Microsoft Excel, and Engineering Equation Solver (EES). WynDyn is the SuperFlow™ computer program that interfaces with the data acquisition system. The raw data was acquired through it and then converted into a spreadsheet to be usable in Excel. Excel was used for aggregating data so that it could be imported to EES. Excel was also used to aggregate and average the output of the EES

calculations and to graph the average results presented in this paper. Engineering Equation Solver (EES) is a computer program designed to give numerical solutions to a set of algebraic equations. EES contains thermodynamic property tables for many fluids including air and water. In EES one can determine the properties of a fluid by providing known data. For example, if supplied the temperature and pressure of a fluid EES will return thermodynamic properties such as enthalpy or entropy. From the properties that EES obtains, performance metrics such as those discussed in the theory section can easily be calculated. An EES code to determine the effects of WFI on the operation of the Model 250-C20B with respect to net power, engine efficiency, component efficiencies, and the concentration of nitrous oxides and unburned hydrocarbons in the exhaust gases was written and is included as Appendix B. This EES code did not seek to model the engine operating with water spray. Modeling the phenomena associated with the operation of the engine with water spray was not the goal of this project; therefore, the computer code that was developed was only for analysis purposes.

IV. Results

There were many interesting consequences of spraying water fog into the compressor inlet of the engine. Insight into the engine operations was also gained in the testing process. The effects of WFI on the Model 250-C20B were classified with respect to net power output, Brake Specific Fuel Consumption (BSFC), component efficiencies, and exhaust gas composition. Table 5 shows data for the operation of the engine with no water spray. The state points match with the state points described in Figure 8. Temperature is denoted by 'T_x', pressure is denoted by 'P_y' and Mach Number is denoted by 'Ma_z'.

Throttle Setting	T_1 (R)	T_2 (R)	T_3 (R)	T_4 (R)	T_5 (R)	P_1 (psia)	P_2 (psia)	P_3 (psia)	P_4 (psia)	P_5 (psia)	Ma_2	Ma_3	Ma_4	Ma_5
75%	530	900	1957	1551	1377	14.7	74	73	25	14.9	0.3	0.033	0.088	0.17
90%	531	979	2194	1752	1465	14.7	94	93	30	14.9	0.29	0.032	0.088	0.20
100%	530	1027	2336	1884	1547	14.7	104	103	33	14.9	0.28	0.032	0.09	0.22

Throttle Setting	Corrected Mass flow rate of air (lbm/s)	Air to Fuel Ratio	Compressor Pressure Ratio	Net Power (Corrected SHP)	BSFC	Concentration of NOX (ppm)
75%	2.8	76.3	5.1	190	0.643	31.6
90%	3.1	61.3	6.3	355	0.515	37.9
100%	3.3	57.2	6.92	420	0.497	42.0

Table 5 Baseline Engine Operation Metrics with No Water Spray

A. Engine Operation during Testing

There were three aspects of the operation of the engine that became apparent during the testing. The first concerns the fuel system. The fuel supplied to the Model 250-C20B is regulated by a governor. The governor operation is driven by the compressor discharge pressure. Higher compressor discharge pressures indicate that the compressor is doing increased work on the incoming air. Higher compressor pressure ratios also indicate that the gas generator turbine-

compressor spool is spinning faster. If the compressor discharge pressure is rising, the rate of change of work done by the compressor and the gas generator turbine is positive. In order to do more work, more energy must be supplied. This necessitates an increased fuel flow rate into the combustor. Therefore, as the compressor discharge pressure increases the governor schedules more fuel to the engine. This relationship is shown in Figure 20. This graph also shows that for a specified pressure ratio increasing the water spray rate caused the fuel flow rate to increase. This means that the relationship between pressure ratio and fuel flow rate was altered when the water spray rate increased.

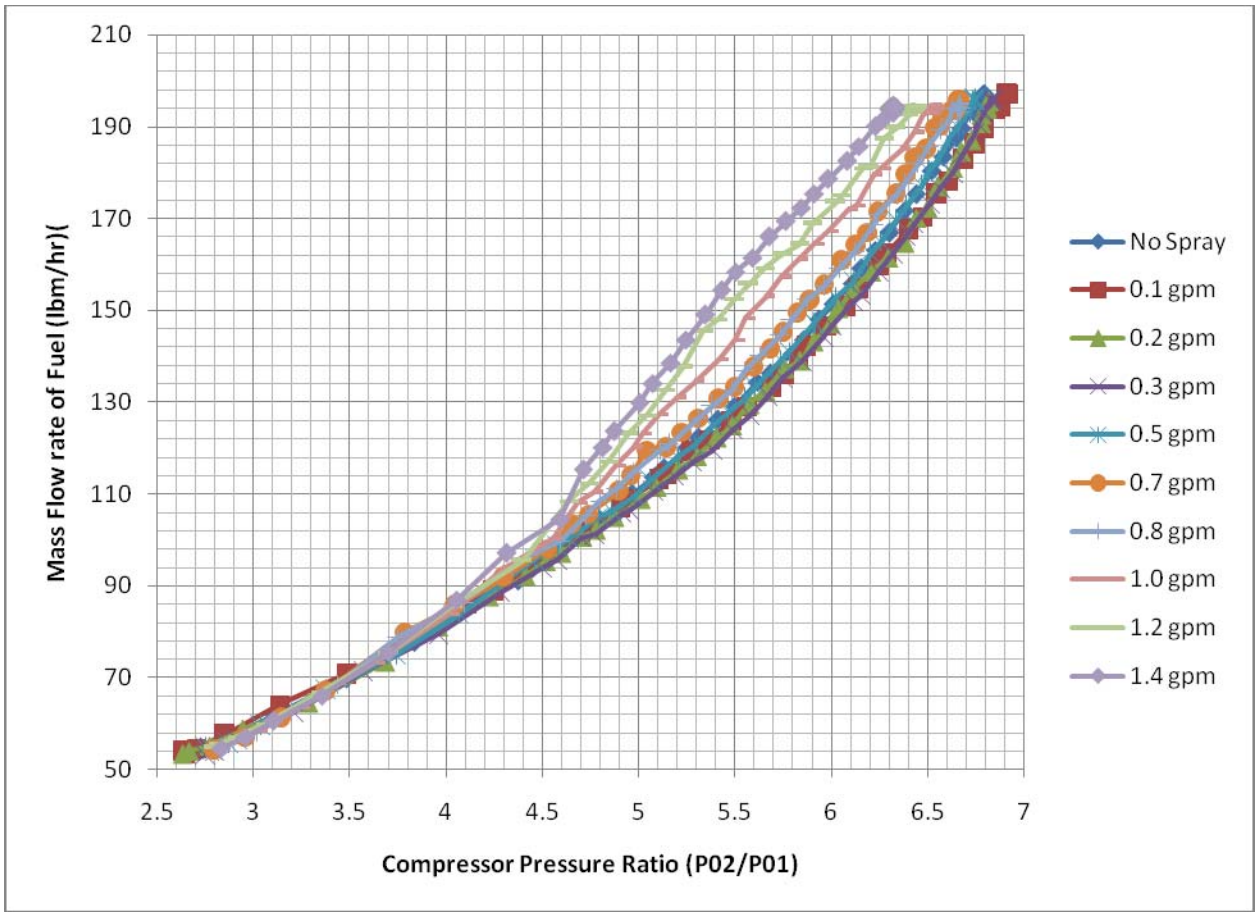

Figure 20 Mass Flow Rate of Fuel vs. Compressor Pressure Ratio.

Figure 20 also shows that there is an engine maximum fuel flow rate and a maximum pressure ratio for each of the water spray rates tested. The fact that this maximum fuel flow rate was the same value for each tested case indicates that the engine is limited to a maximum fuel flow through a limitation device on the fuel pump. The pressure ratio when maximum fuel flow rate occurs for the no spray run is the quoted maximum pressure ratio for the engine, 7:1. This indicates that this maximum fuel flow was a designed limit. It can also be seen that the maximum fuel flow is reached at a lower pressure ratio for increasing water spray rates. This indicates that the higher water flow rate tests were not supplied with sufficient fuel to reach the full potential pressure ratio of the engine.

Many trends of the comparison metrics investigated were also limited. This is not due to the thermodynamic principles of the effect of WFI, but is due to the fact that at higher water spray rates the engine becomes limited by fuel flow rate. As was noted above, this point of maximum fuel occurs differently for each water spray rate. For this reason, the trends must be considered and not only the maximum or minimum values for each parameter.

As was noted earlier, the bleed valve operates during the start up stages of the engine's operation. It was only after water spraying began and water was seen coming out of the valve was its operation understood. When the valve is open from 65% throttle to 72% throttle and water is being sprayed, water comes out of the bleed air valve. This means that not all of the water goes though the engine. Unfortunately this means that in the presented results, the portion of a test that occurs before the bleed air valve has closed is not representative. To fully understand the effects of the WFI on the engine, one should consider only the portion of the results that occur after the bleed air valve has closed. The information that described when this occurred for different metrics was provided in Table 4 for the No Spray case. The portion of the

tested results for the time when the bleed air valve was open is still presented because it represents the actual operation of the engine under the effects of Water Fog Injection.

Ambient atmospheric conditions can affect the operation of a gas turbine engine. Most of the tests were conducted over a span of a few days. Two of the water spray rate tests were performed apart from the others: the 0.1 gpm runs and the 0.2 gpm runs. All of the runs for these two flow rates were conducted over two days. The results for each of these tests are also different than results for the tests with 0.3 or more gallons per minute of spray. These data don't really follow the same trends as the rest of the flow rates with respect to how metrics changed with increasing water spray rates. The greatest difference between the 0.1 gpm and 0.2 gpm runs and the water spray tests greater than 0.3 gpm concerns the mass flow rate of air through the engine. The raw data for the flow rate of air was corrected so that it would represent what the corrected flow rate would be at sea level, but the 0.1 gpm and 0.2 gpm corrected flow rates were higher than for the other runs. For this reason, when a performance metric is plotted against the mass flow rate of air, different trends appear for the 0.1 gpm and 0.2 gpm runs. The cause of these differences is unknown. It is known that the ambient air temperature was slightly warmer for the 0.1 and 0.2 gpm days. Additionally, the 0.1 gpm and 0.2 gpm tests used the smaller capacity spray nozzle exclusively, while the other water spray rates used the larger capacity nozzle exclusively. A difference in spray characteristics, i.e. droplet size distribution, between the runs is another possible cause for the difference in results.

The overall effect of WFI on the engine power is presented before effects of WFI on individual components of the engine. Increasing rates of water spray increased the net power of the engine for a specified corrected mass flow rate of air. This trend can be seen in Figure 21. However, the effects of fuel limitation and pressure ratio for increasing water spray rates are also

depicted. Specifically, it can be seen that the engine makes less power at wide open throttle setting for the higher water spray rates.

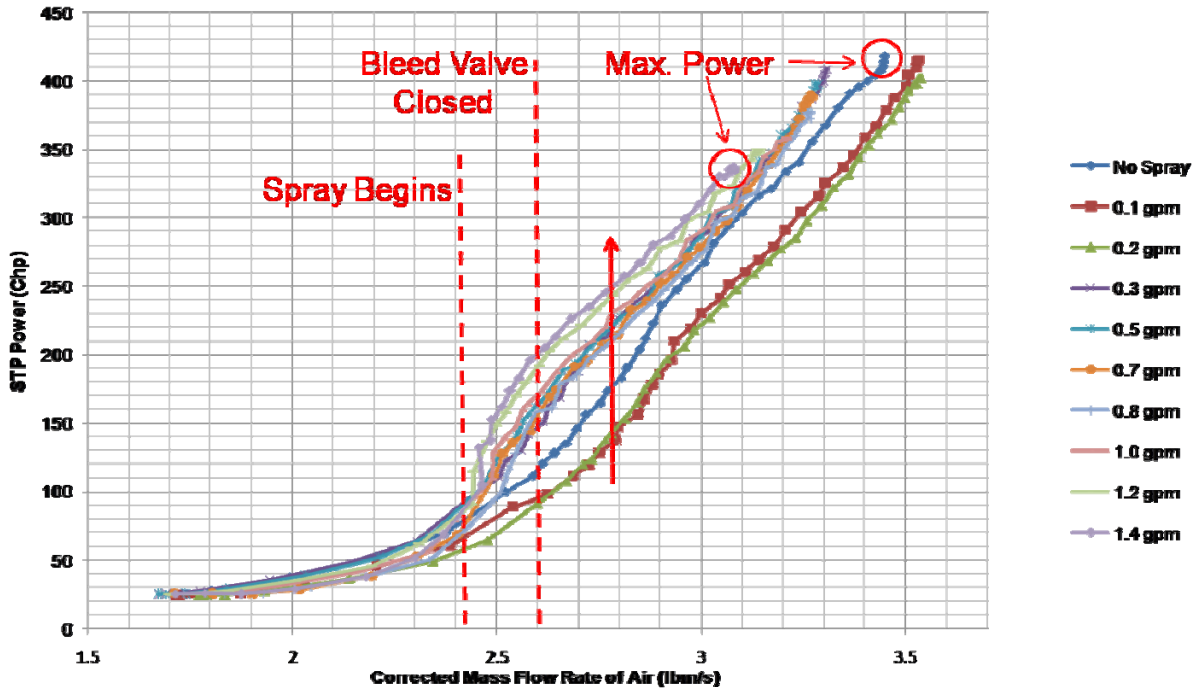

Figure 21 STP Power vs. Corrected Mass Flow Rate of Air

B. Effects of WFI on the Compressor

The effects of WFI on the engine and its components are presented beginning with the compressor. Water Fog Injection causes the compressor to perform better. This involves improvements in pressure ratio and isentropic efficiency with increasing water spray rates. Figure 22 shows the compressor pressure ratio vs. the gas generator turbine/ compressor speed. The speed is the same for both components as they are connected via a shaft. This graph shows the expected trend that as compressor speed increased the pressure ratio increased. The graph also shows that for a specified compressor speed as the water spray rate increased compressor

pressure ratio increased. This means that at a constant speed increasing the water spray rates caused the compressor discharge pressure to increase. This means that the compressor performs better with WFI than it does with no spray.

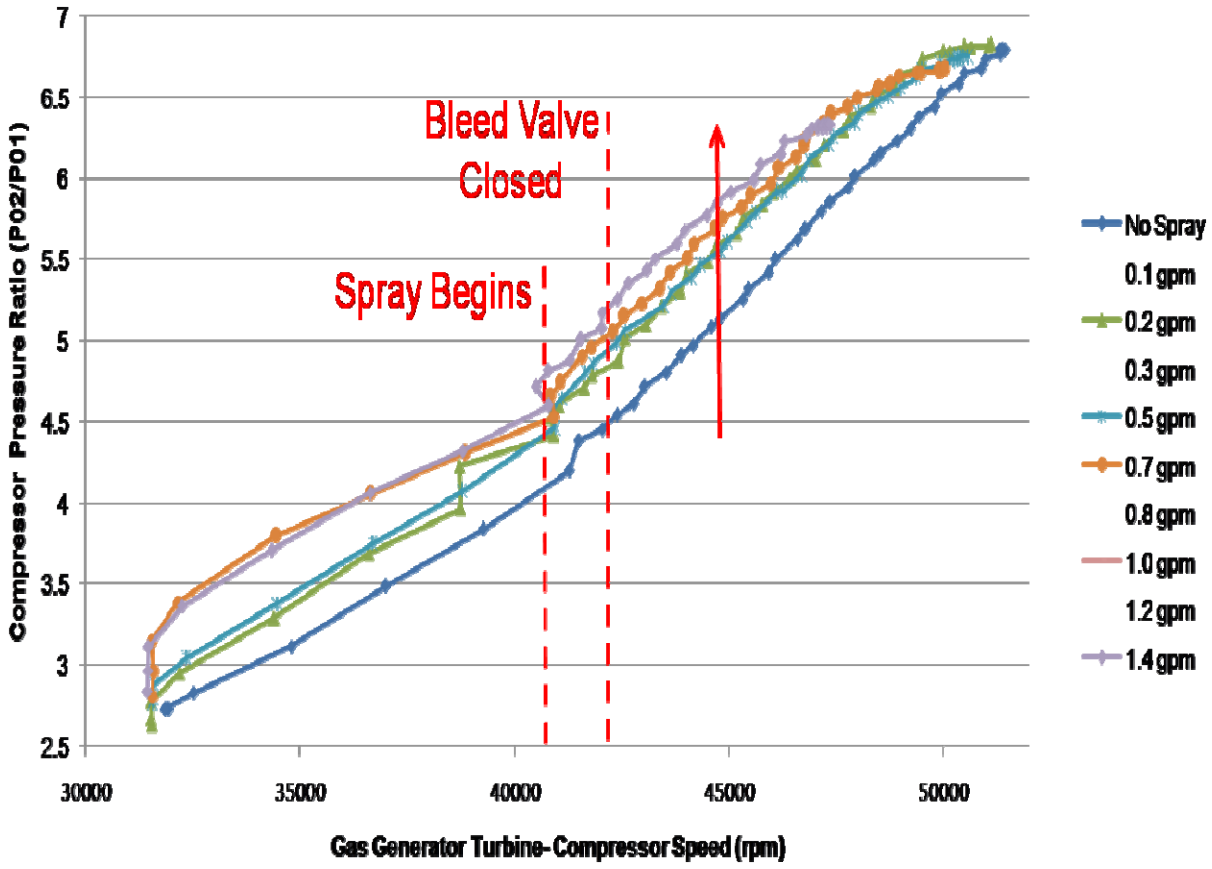

Figure 22 Compressor Pressure Ratio vs. Compressor Speed

Because the compressor achieved a higher pressure ratio for a given compressor speed, the mass flow rate of air through the engine increased with respect to compressor speed as water spray rate increased. The two aspects for increasing the power of the engine are increasing the mass flow rate through the engine for a specific operating point, and increasing the specific work of the power turbine. The increased mass flow rate of air means that there more mass is available to carry more energy through the engine contributing to the increase in power. Figure

23 depicts pressure ratio across the compressor vs. the corrected mass flow rate of air, a gas turbine industry standard comparison.

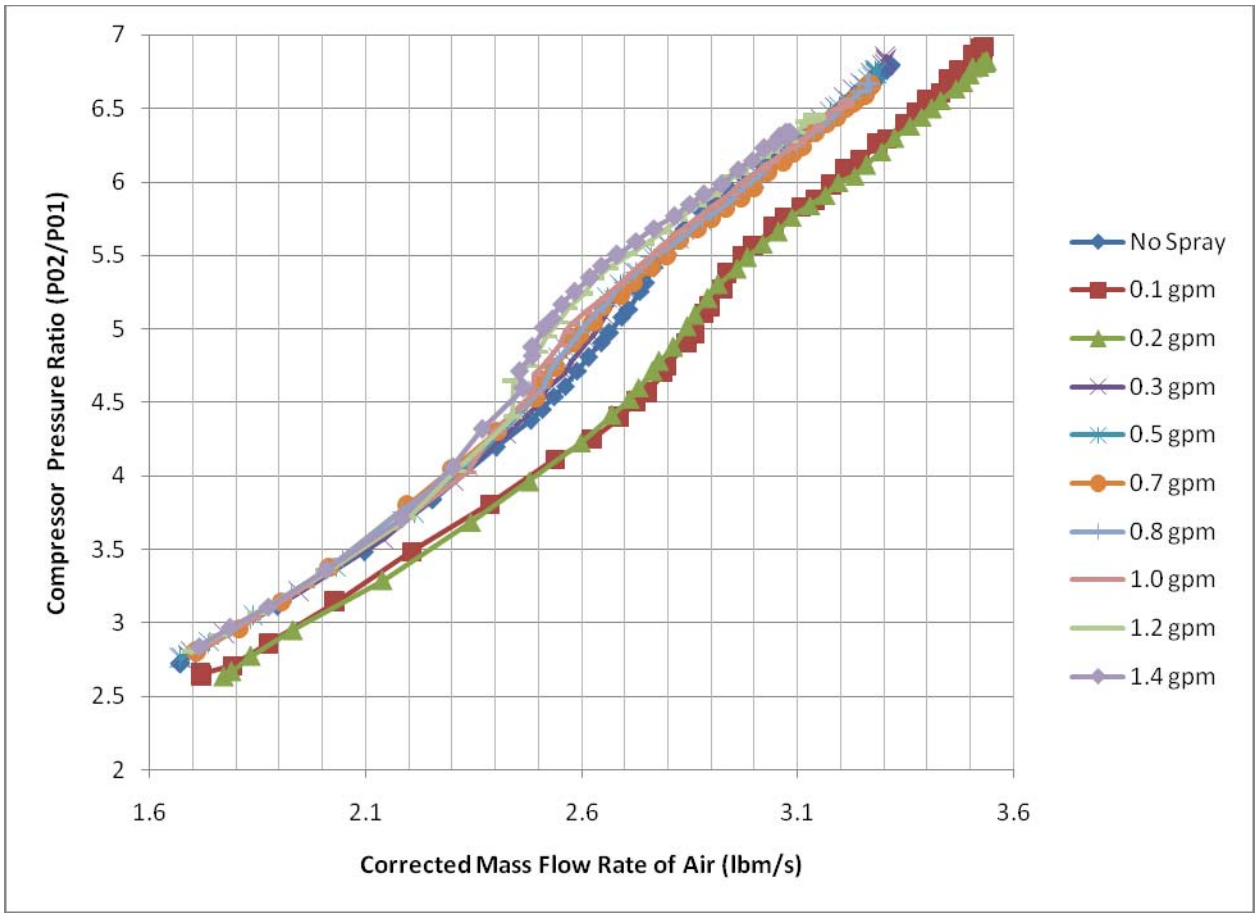

Figure 23 Compressor Pressure Ratio vs. Corrected Mass Flow Rate of Air

One purpose of spraying water into the engine was to cool the air as it goes through the compressor in order to minimize the compressor work. It was determined that the water did in fact cool the air as it passed through the compressor. Figure 24 shows that as the water spray flow rate increases the temperature at the compressor discharge decreased. This was because the water absorbed energy and lowered the compressor discharge temperature of the air water vapor mixture. The solid black line in Figure 24 denotes the saturation temperature of water for a given pressure, as represented by the pressure ratio. A temperature above this line would

indicate that water in these conditions would likely be a superheated vapor. A temperature below the saturation line would indicate that water in these conditions would be a subcooled liquid. This indicates that for at least the runs of 0.8 gpm through 1.4 gpm the water has not vaporized before it reached the compressor discharge.

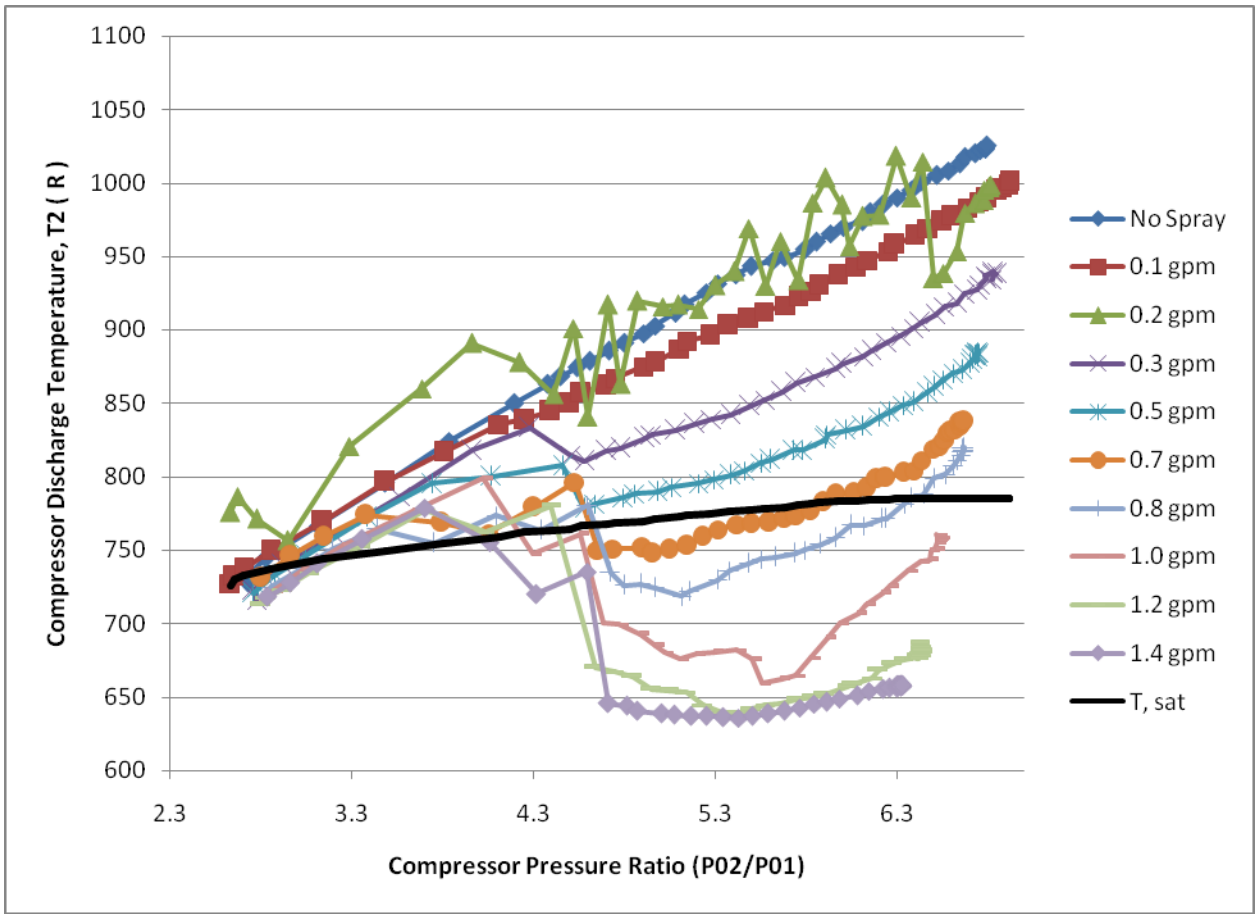

Figure 24 Compressor Discharge Temperature vs. Compressor Pressure Ratio

For a compression process where the water stays a subcooled liquid, the process is not the compression process of a gas mixture, but the compression process of a mixture that has a gas component and a liquid component, that is wet compression. Simplified heat transfer calculations were performed for the heating of a droplet in the compressor. These calculations can be found as Appendix D. The solution is a difficult one without simplifying assumptions. It

was assumed that the droplet remained constant in diameter and temperature throughout the process. It was also assumed that the droplet was exposed to air at an average temperature and pressure for the compressor. The amount of time needed for the hot air to transfer enough energy to the droplet to vaporize the droplet was compared with the amount of time the droplet spent in the compressor. It was determined that even at low water flow rates there is insufficient time for a droplet to fully vaporize. As mentioned, these calculations were rudimentary, and a full treatment of this problem was better suited for a future investigation. For this reason, the conclusions based on the calculations only descirbe the probable trend. This trend is that the droplets did not acquire enough energy in the time they spent in the compressor and therefore, there was the possibility that with a flow rate below 0.8 gpm the water has not fully vaporized in spite of the local temperature and pressure. All of these estimates together mean that there is a high probability that wet compression took place in the compressor at even moderate water spray rates, which could have had a limiting effect on the capabilities of the engine. The effects of wet compression for lower pressure ratio gas turbine compressors will be examined at a later date as part of the recommendations for further study.

The presence of water spray also effected the compressor's isentropic efficiency. Figure 25 shows the relationship between the compressor isentropic efficiency and the pressure ratio across the compressor. The average efficiency for the runs with no spray and spray up to 0.2 gpm stayed fairly constant across the operating range. However, with higher water spray flow rates the efficiency began to respond more to the presence of the water spray. For the spray rates of 0.3 gpm to 1.0 gpm, the compressor efficiency increased along with the pressure ratio, but reached a maximum and began to decline before the pressure ratio reached its maximum. For

the 1.2 gpm and 1.4 gpm runs the efficiency increased with respect to the pressure ratio for the entire operating range of the engine.

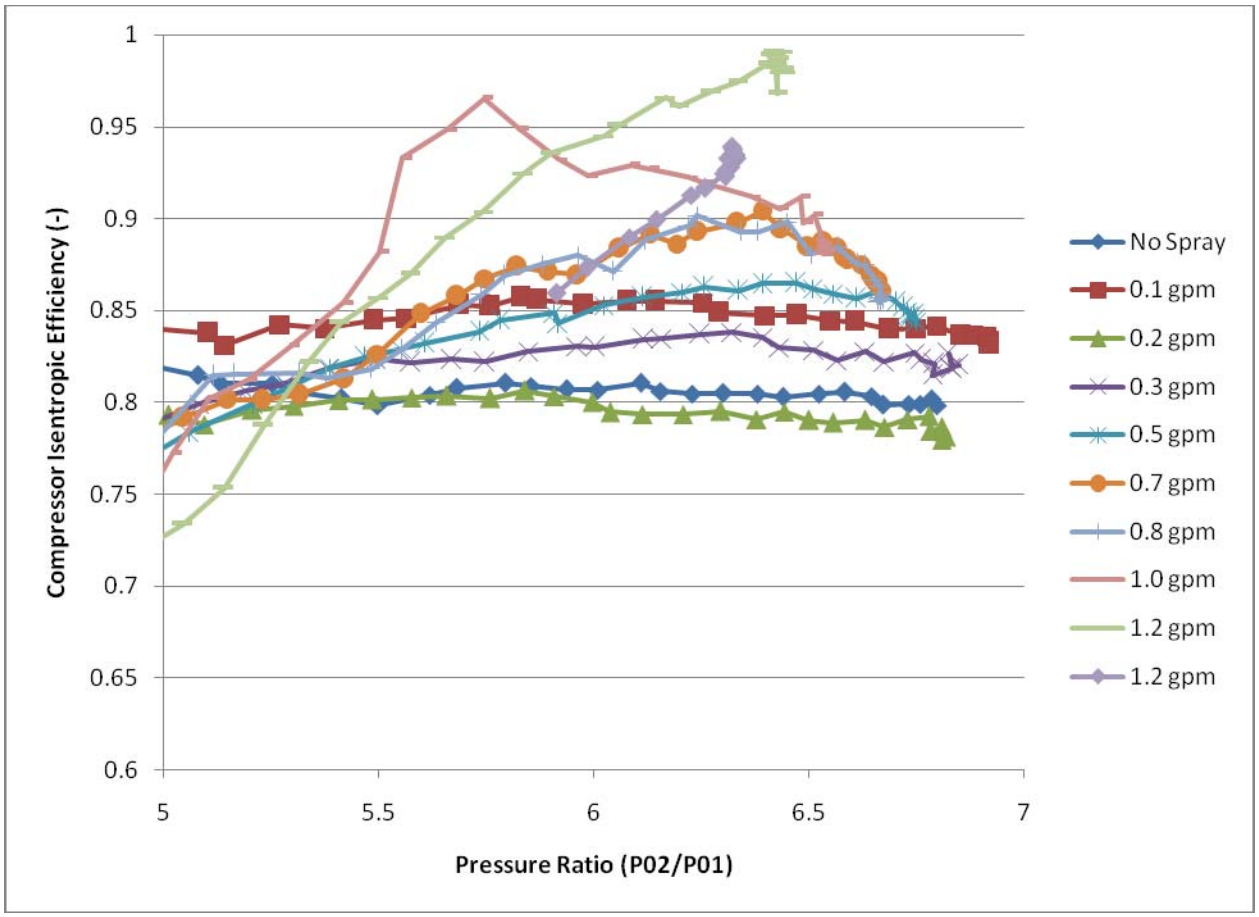

Figure 25 Compressor Isentropic Efficiency vs Compressor Pressure Ratio

The bleed air valve was open until a mass flow rate of about 2.7 lbm/s was achieved. This meant that some of the water spray left the engine before reaching the thermocouples in the compressor discharge. The amount of water that escaped the engine was unknown; therefore, it was not possible to not try and account for the losses in the analysis model. Therefore, the calculated compressor efficiencies in this range are inaccurate and are not considered in the analysis.

C. Effects of WFI on the Combustor

Figure 26 shows that for a given mass flow rate of air, increasing water spray flow rate causes the combustor temperature to decrease significantly. The maximum temperarture achieved in the combustor at the 3.1 lbm/s mass flow rate of air with no spray was 2090 Rankine where as the average maximum temperature for the 1.4 gpm runs was 1940 R. This drop of about 150 degrees is significant when one considers that the the gas turbine engine produces power by converting the heat of the hot gas mixture of the combustion reaction into mechanical energy through the mechanical conversion of spinning the turbines. This decrease in temperature for a specifed mass flow rate of air contributed to the effects that WFI had on the compostion of the exhaust gases.

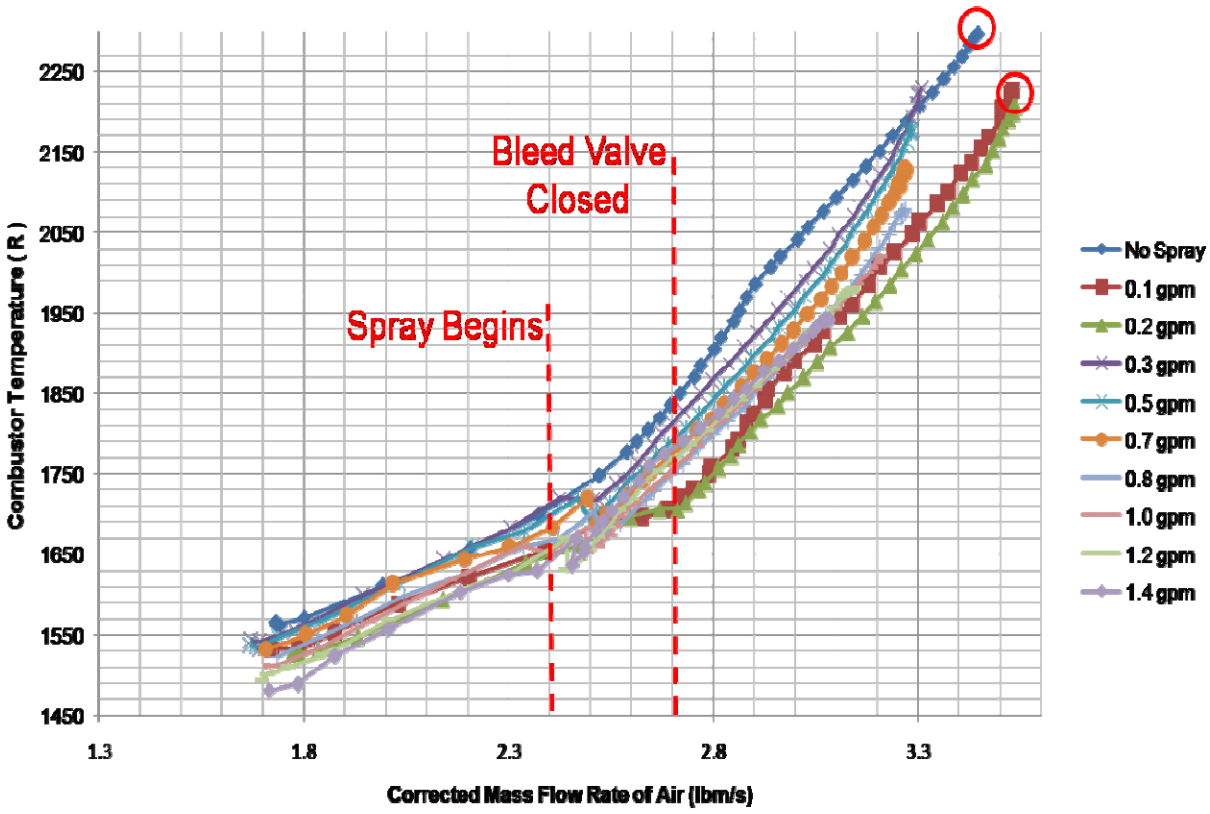

Figure 26 Combustor Temperature vs. Corrected Mass Flow Rate of Air

D. Effects of WFI on the Gas Generator Turbine

WFI affected the gas generator turbine's pressure ratio and efficiency. Figure 27 shows the corrected mass flow rate of air vs. the pressure ratio across the gas generator turbine. The pressure ratio across the GGT for a given corrected mass flow rate of air was higher for increasing water spray rates. This trend is directly related to the compressor pressure ratio's trends. The GGT pressure ratio was higher inpart due to the fact that the compressor required more power because is did more compression work on the air.

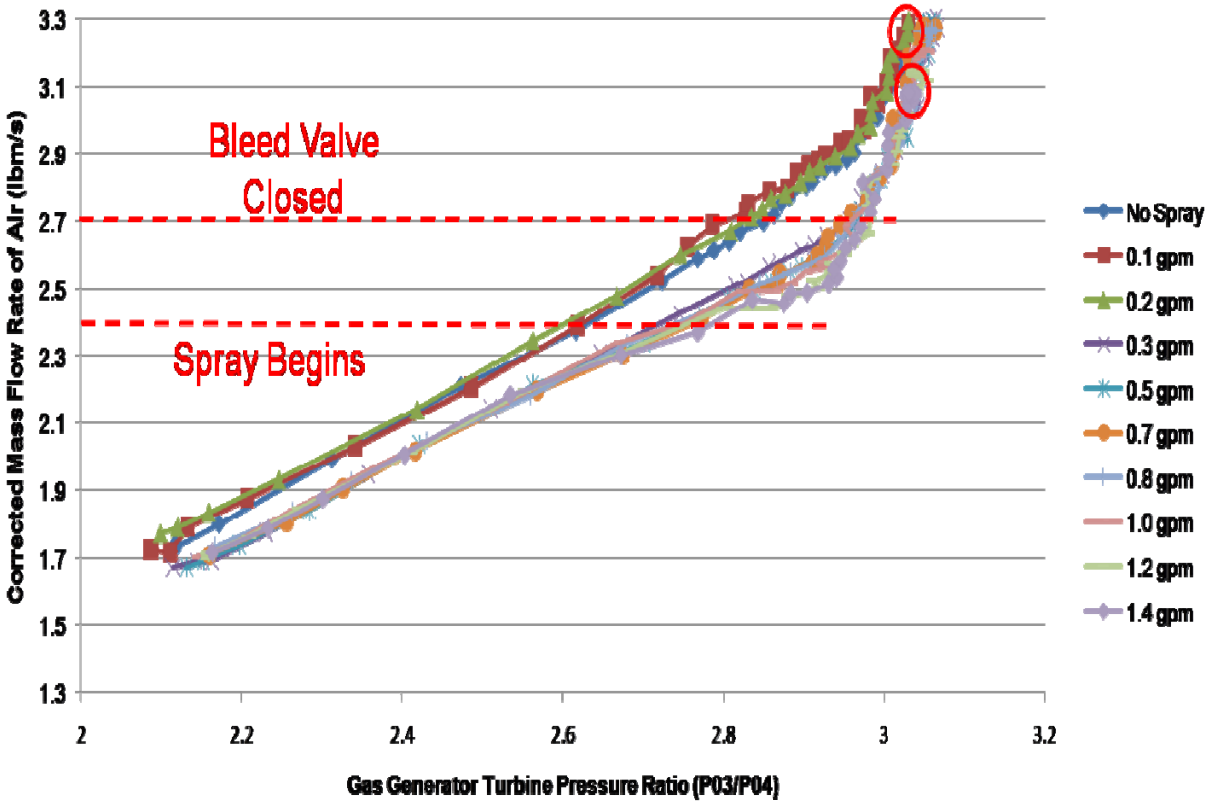

Figure 27 Corrected Mass Flow Rate of Air vs. GGT Pressure Ratio

The Gas Generator Turbine Isentropic efficiency was also affected by the water spray. Figure 28 shows the relationship between the GGT Isentropic Efficiency and the Corrected Mass

Flow Rate of Air for varying water spray rates. The general trend shown is that, except for the 0.1 and 0.2 gpm tests, lower flow rates of water spray increased the efficiency. However, higher water spray rates caused the efficiency to decrease below the level of the no spray runs.

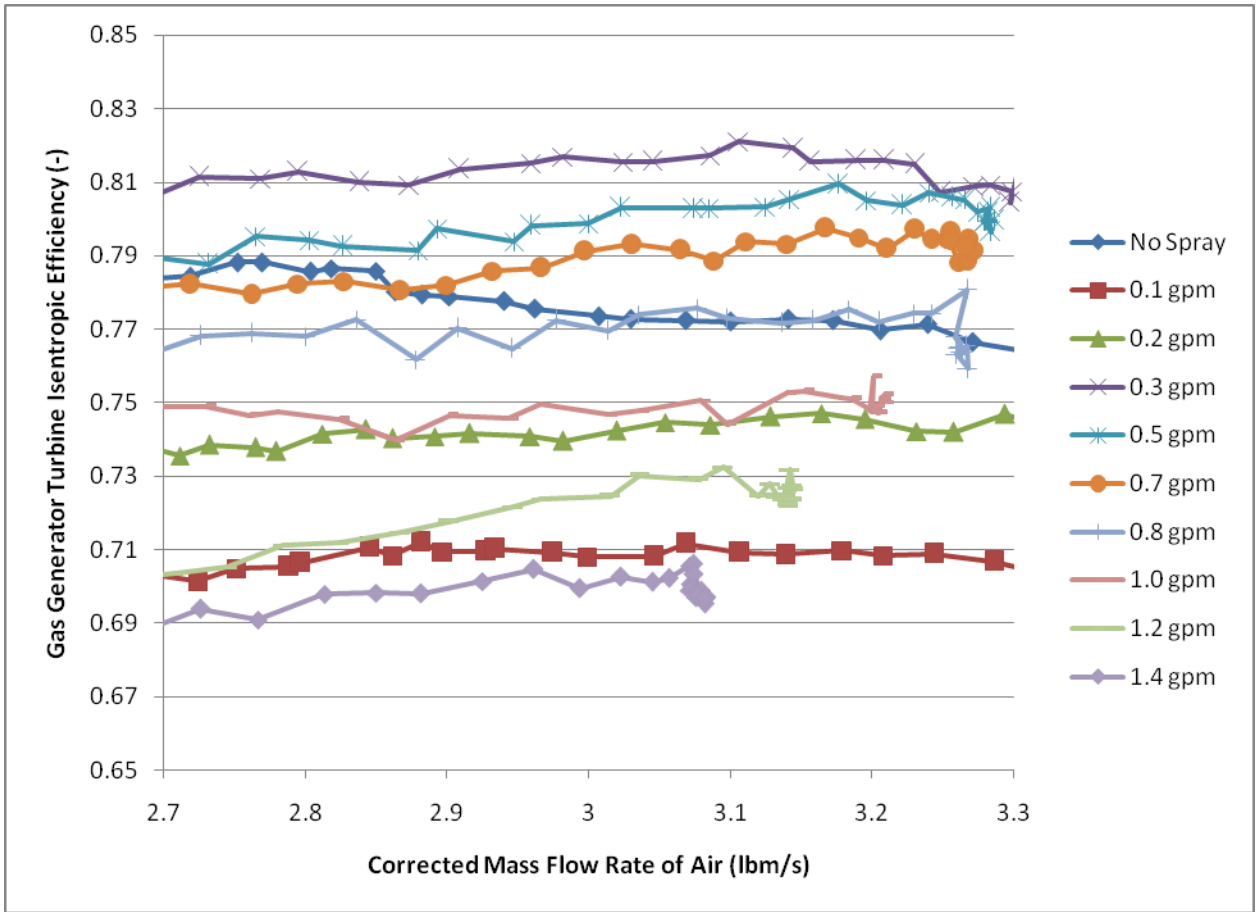

Figure 28 GGT Isentropic Efficiency vs. Corrected Mass Flow Rate of Air

E. Effect of WFI on the Power Turbine

Increasing water spray rates also affected the operation of the power turbine, including the pressre ratio and the isentropic efficiency. From Figure 29 it is seen that increasing water spray rates caused the pressure ratio across the power turbine for a specified air flow rate to increase. This means that there was a higher pressure ratio across the power turbine for the hot

exhaust gases to expand through. This directly contributed to the increased net power for a specifed air flow rate that WFI caused.

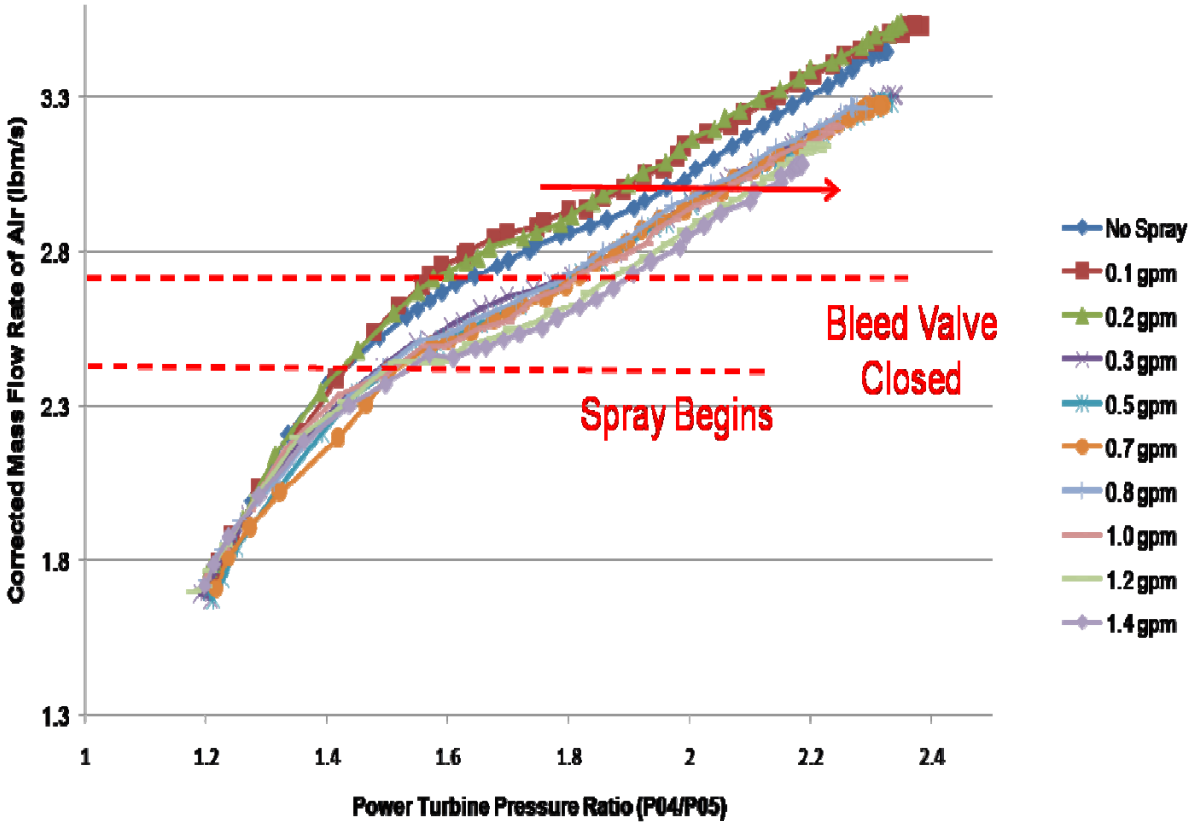

Figure 29 Corrected Mass Flow Rate of Air vs. Power Turbine Pressure Ratio

Figure 30 shows the power turbine isentropic efficiency vs. corrected mass flow rate of air. The trend was similar to that of the GGT isentropic efficiency. Increasing the water spray rate initially caused the efficiency to decrease for a given air flow rate. After 0.7 gpm of water flow, though, the efficiency began to increase as water spray rate increases.

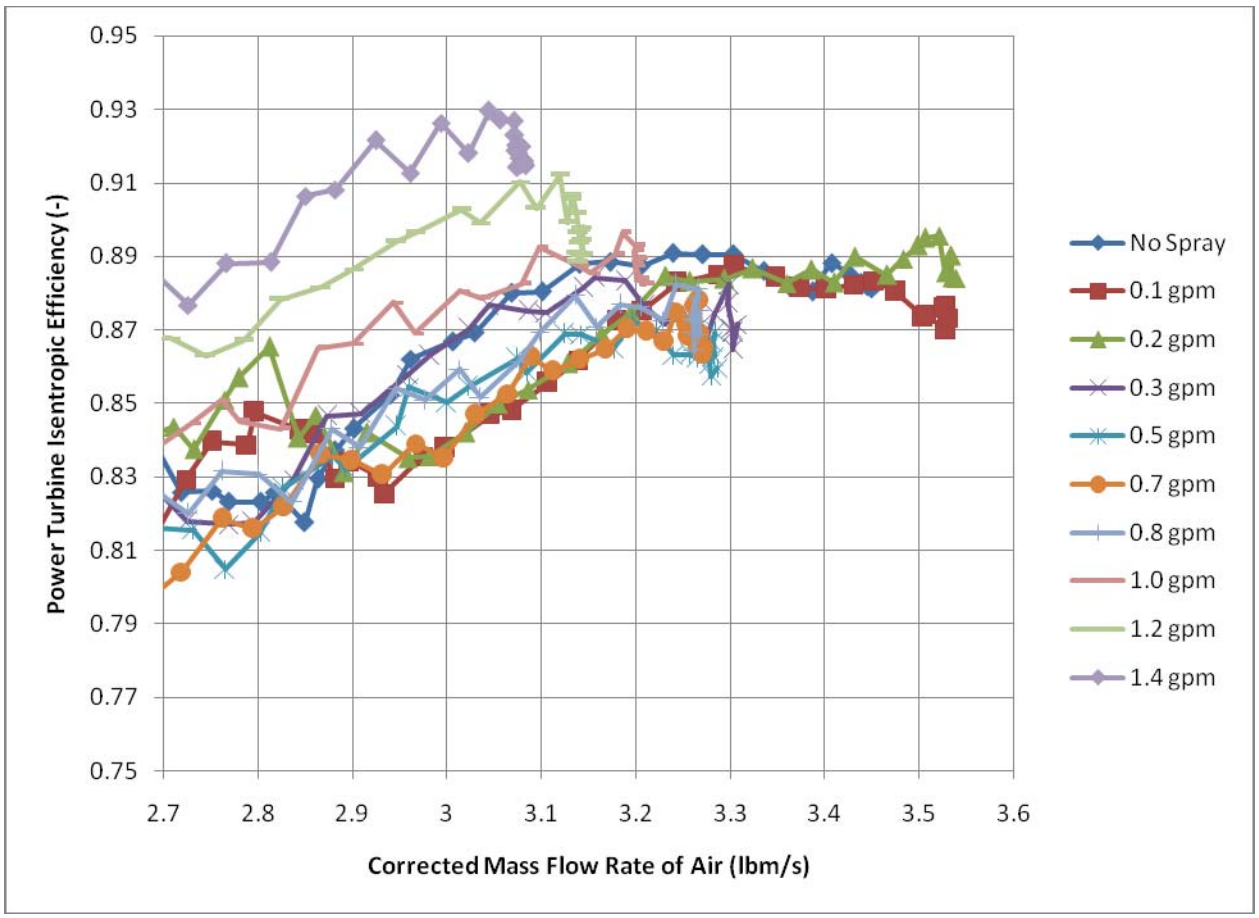

Figure 30 Power Turbine Isentropic Efficiency vs. Corrected Mass Flow Rate of Air

F. Effect of WFI on Emissions

As mentioned in the introduction, one of the reasons that water fog injection is used in larger gas turbine engines is to decrease the concentration of Nitrous Oxide (NO_x) emissions. The presence of water spray in the engine affected the composition of the exhaust gases, especially the NO_x concentration. From the No Spray line in Figure 31, the Concentration of Nitrous Oxides vs. Combustor Temperature, it can be seen that as the combustor temperature (which is synonomous with engine power) increases, the concentation of NO_x increases. As was shown earlier, increasing water spray rates caused the combustor temperature for a given

operating point to decrease. This decrease in temperature significantly affected the NO_x concentration and is shown in Figure 31. The 0.1 gpm and 0.2 gpm spray rates decreased the concentration of NO_x for a given temperature over the base 'no spray' test, but the general trend of increasing NO_x concentration with combustor temperature was still present. The water spray rates of 0.3 to 1.4 gpm led to an almost flat response in terms of NO_x concentration. This marks a 36% decrease in the concentration of nitrous oxides in the exhaust gases at maximum power.

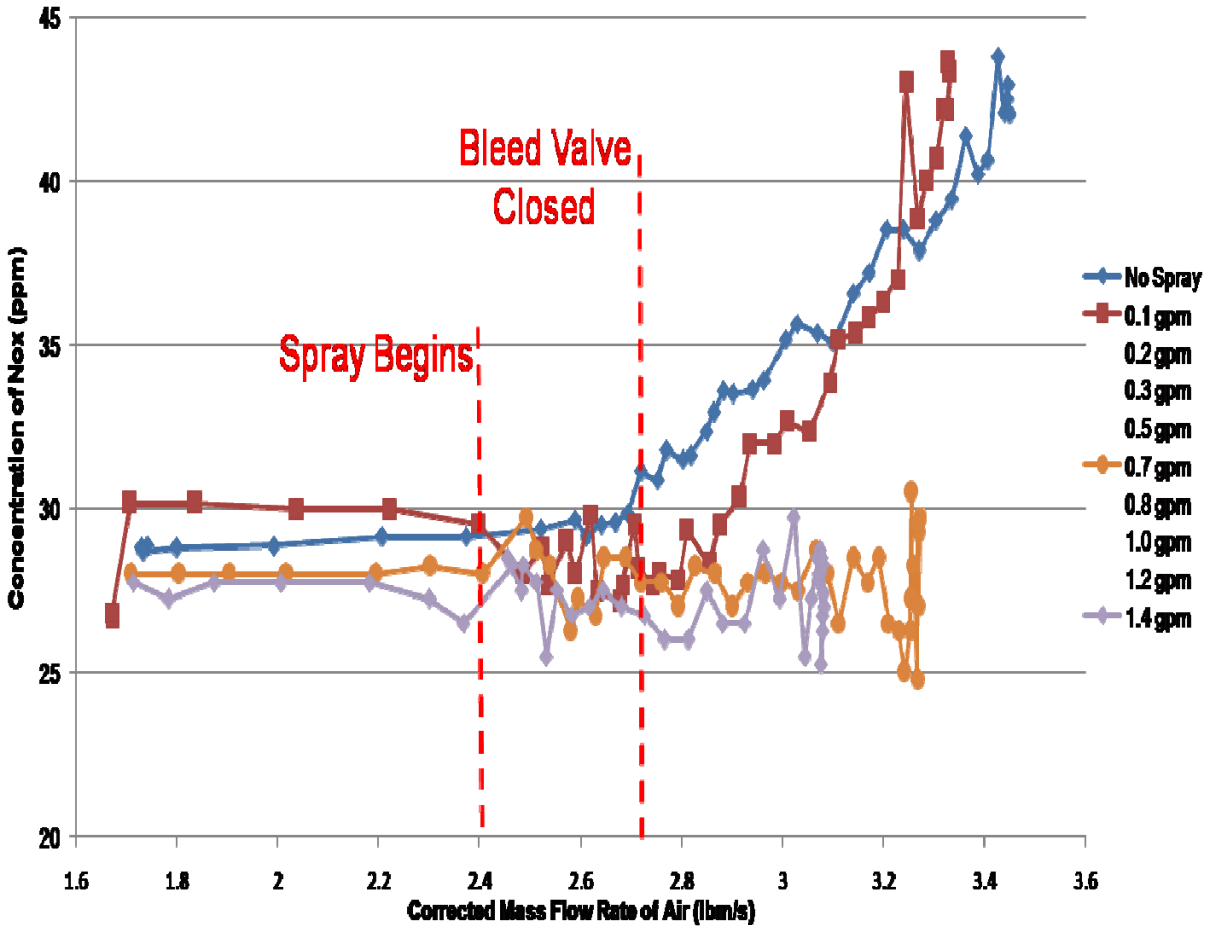

Figure 31 Concentration of NO_x vs. Combustor Temperature

Because the data is very noisy, least squares regression lines were fit to the data. The product of this operation can be seen as Figure 32. Once the least squares regression is considered, it can be seen that the presence of water spray above 0.2 gpm caused the

concentration of nitrous oxides to average out to around 27.5 ppm. For reference, the combustor tempature that corresponds to the initiation of the water spray is 1710 R for the No Spray runs. This is approximately the same tempreature for each run. For the higher water spray rates, the NO_x concentrations before and after water spray were initiated are almost identical.

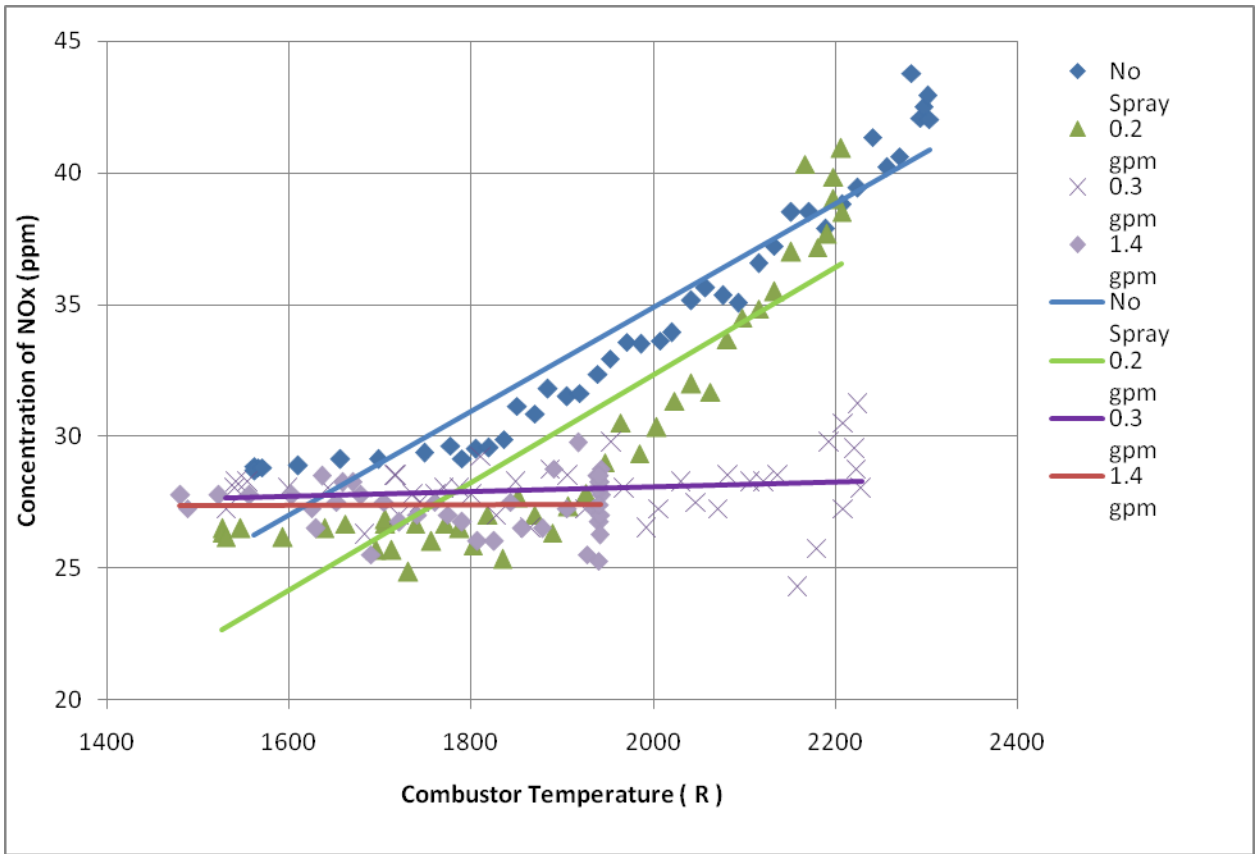

Figure 32 Least Squares Regression of NO_x Concentration vs. Combustor Temperature

Unburned hydrocarbons are another important part of the exhaust gases. A higher concentration of unburned hydrocarbons would indicate that the combustion process is not complete. Figure 33 shows the relaionship between the unburned hydrocarbons and the combustor temperature. The least squares regression of the data in Figure 33 is included in Figure 34 for ease of analysis.

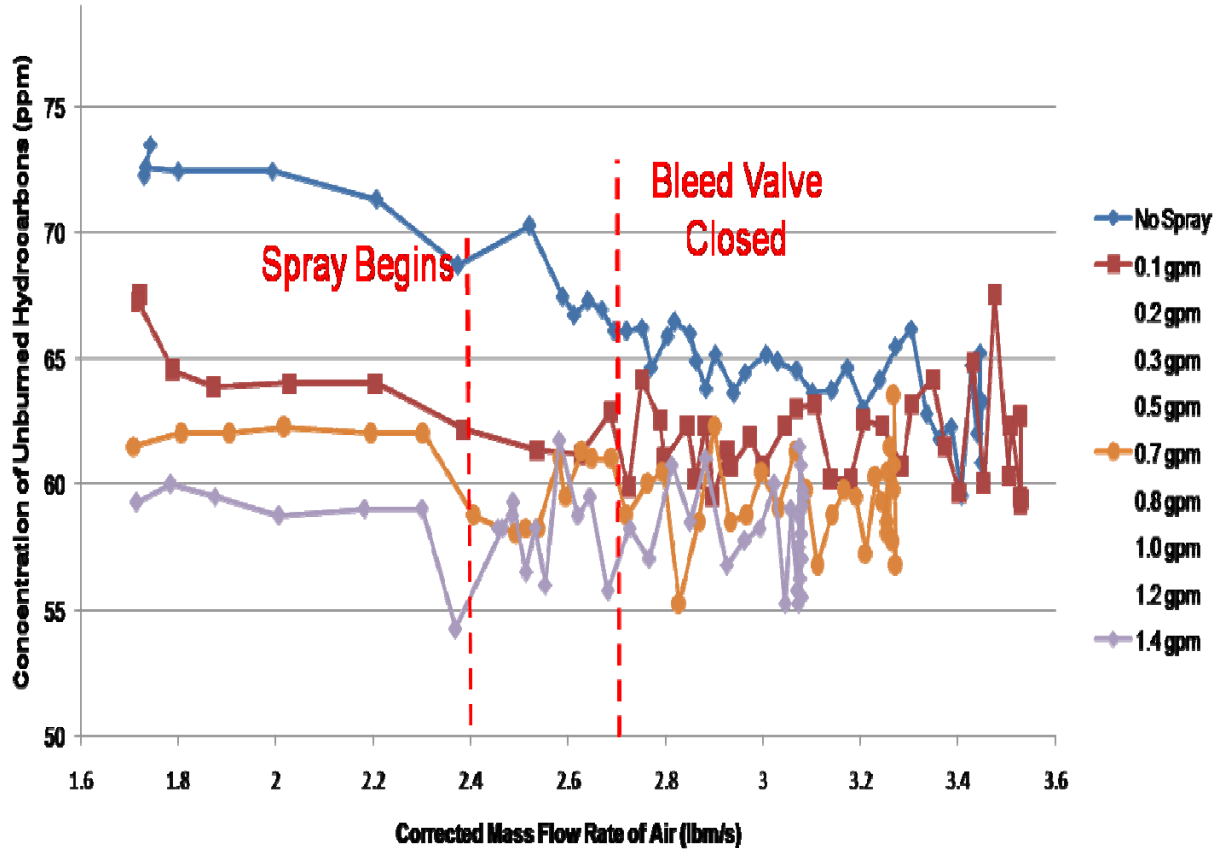

Figure 33 Concentration of Unburned Hydrocarbons (HC) vs. Combustor Temperature

The general trend for the no spray tests was that the amount of unburned hydrocarbons would decrease as the combustor temperature increased. Increasing water spray rate tended to decrease the concentration of unburned hydrocarbons. The largest difference, though, occurred between the no spray runs and the initial application of water spray. The water spray changed the basic relationship between the concentration of the of unburned hydrocarbons and temperature. For a fixed combustor temperature, increasing the water spray decreased the concentration of unburned hydrocarbons. The greatest difference was at lower throttle settings where 1.4 gpm achieved a 16% decrease in the concentration of unburned hydrocarbons over the

no spray test. At maximum throttle settings, 1.4 gpm only achieved an 8% decrease in the concentration over the no spray test.

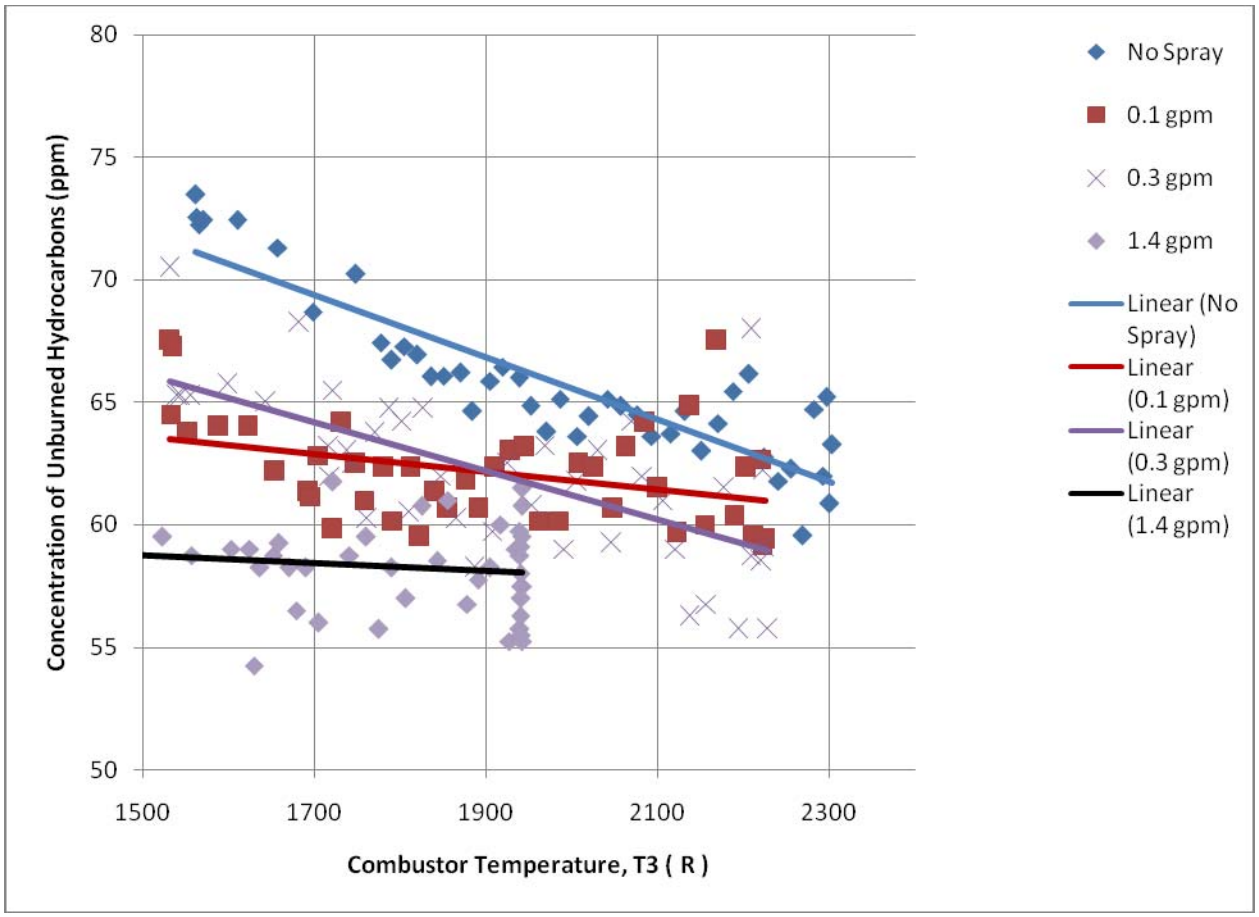

Figure 34 Least Squares Resgression of Concentration of HC's vs. Combustor Temp.

G. Effects of WFI on Net Power

It was discussed earlier that WFI caused the net power to increase for a specified mass flow rate of air. Figure 35 shows that increasing water spray rates also increased the net power with respect to a specified combustor temperature. At a combustor temperature of 1940 Rankin the 1.4 gpm test shows a 68% increase in net power over the baseline no spray test. The trends in this graph show that if the combustor temperature could be increased further significant power

gains could be achieved. In the normal operation of the engine, the combustor temperature is the limiting factor of the maximum producible net power. The combustor temperature is limited because of material limits of the engine itself. The materials that make up the combustor and the turbine blades are only able to withstand limited temperatures before failing. Figure 35 shows how the maximum power of the engine can be increased without increasing the maximum combustor temperature. If the fuel flow rate were not limited, the maximum combustor temperature in the no spray test of 2300 Rankin could be reached in the 1.4 gpm spray test. If the trends between combustor temperature and net power remained the same for 1.4 gpm spray at elevated temperatures, then, at 2300 Rankin the 1.4 gpm test case would produce 570 SHP. This would be a 36% increase over the baseline no spray test.

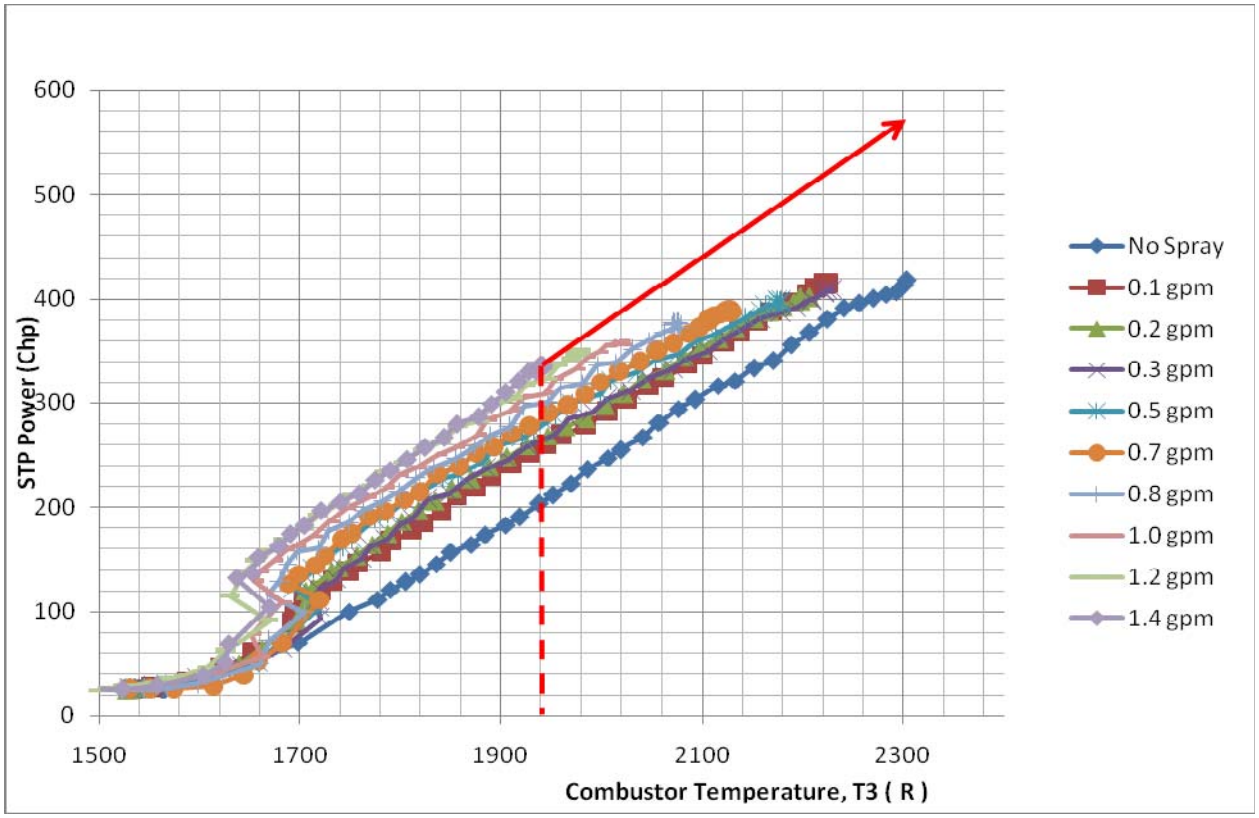

Figure 35 STP Power vs. Combustor Temperature

H. Effects of WFI on BSFC

Though the fuel flow rate has already been discussed, it will be touched on again as the effects of water spray on the Brake Specific Fuel Consumption (BSFC). The BSFC is a measure of efficiency. It is the ratio of fuel flow rate to the net power. Figure 36 shows the relationship between BSFC and the STP Corrected Power for the varying water spray rates. Figure 36 shows the general trend for normal operation that BSFC decreases as the net power increases, meaning that the fuel efficiency increases. However, Figure 36 also shows that as the WFI rate increased the Brake Specific Fuel Consumption increased. This indicates that as WFI rate increased overall cycle efficiency decreased. Figure 37 shows the same data as Figure 36 but with the focus on the power levels corresponding to normal operation.

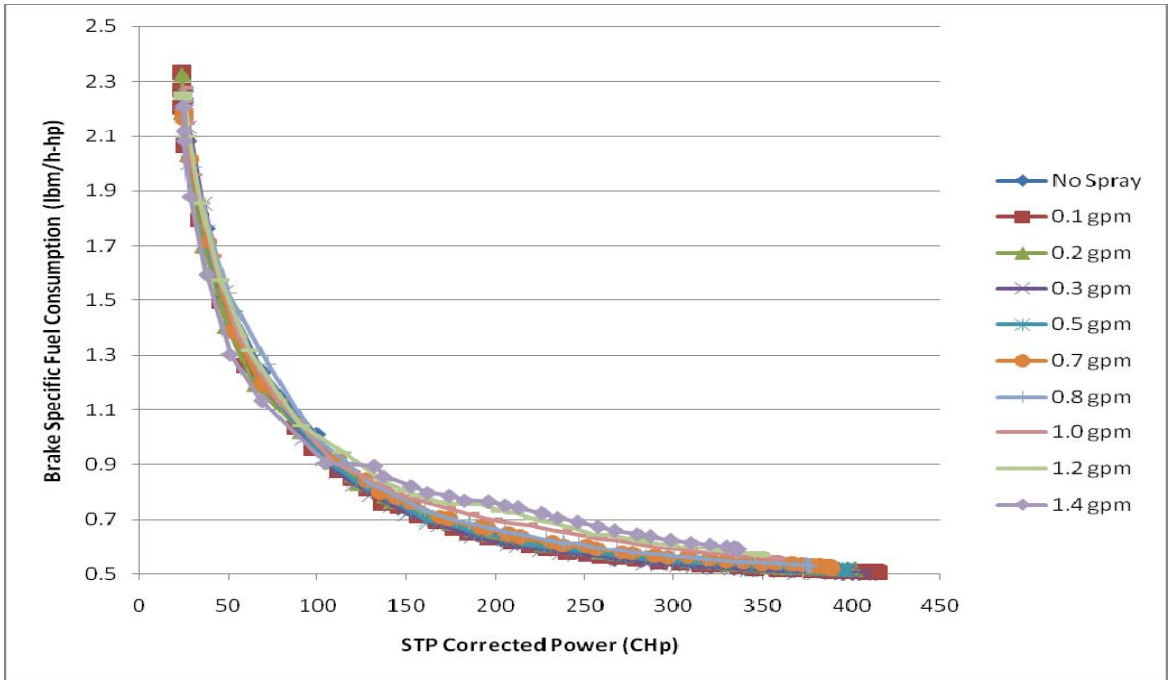

Figure 36 Brake Specific Fuel Consumption (BSFC) vs. STP Corrected Power

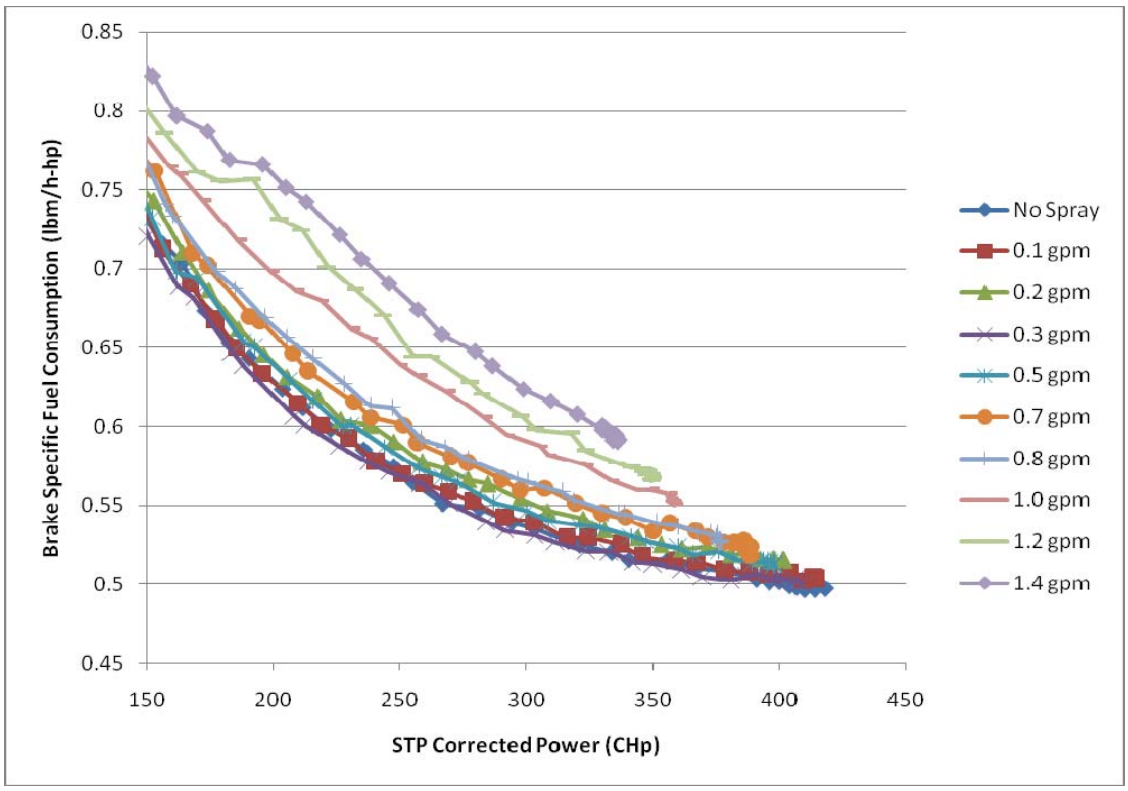

Figure 37 Brake Specific Fuel Consumption (BSFC) vs. STP Corrected Power (Focused on the relevant area)

In Figure 37 it is shown that the normal operating trend of decreasing BSFC with increasing power holds for the all tests. It also shows that as WFI rate increases BSFC increases. This indicates that with water spray the engine is less fuel efficient.

V. Conclusions

Water Fog Injection significantly affects the performance of the Model 250-C20B. WFI affected both the physical and thermodynamic operation of the engine. WFI caused the temperature at the compressor discharge to drop significantly. Spraying water into the engine also profoundly affected the operation of the engine's governor. This caused more fuel to be used sooner in the throttle range, which in turn caused the engine to reach maximum fuel flow well before it was expected. The limited fuel flow rate limited the extent of the investigation.

The inclusion of water in the working fluid of the engine also lowered the combustor temperature.

In spite of limited fuel flow, WFI increased net power of the Model 250-C20B for a given mass flow rate of air. This effect increased as the rate of WFI increased. The maximum improvement over the baseline occurred for the 1.4 gpm test at 67% higher power at a combustor temperature of 1940 Rankin. If an unlimited supply of fuel had been available, this trend would have likely continued until the engine reached its operational limiting combustor temperature. This would have resulted in a maximum net power of the engine that was 36% higher than the baseline operation.

WFI also decreased the concentration of nitrous oxides and unburned hydrocarbons in the exhaust. The WFI rates of 0.1 and 0.2 gpm slightly reduced the concentration of NO_x in the exhaust, but the concentration continued to increase as combustor temperature increased. All WFI rates of 0.3 gallons per minute or greater reduced the concentration of NO_x by 36%. These WFI rates not only decreased the concentration of NO_x, it completely altered the relationship between the concentration of NO_x in the exhaust and throttle setting. For these WFI rates, the concentration of NO_x was approximately the same at all throttle settings. The effects of WFI on the concentration of unburned hydrocarbons in the exhaust were more modest. All WFI rates showed some decrease in concentration of unburned hydrocarbons, but none very significant. The 1.4 gpm test only decreased the concentration by 16% at low throttle settings over the no spray test and 8% at high throttle settings.

WFI caused increases in Brake Specific Fuel Consumption (BSFC) for all WFI rates. For a specific power setting, increasing WFI rates increased the BSFC. The 1.4 gpm test caused an 11% increase in BSFC over the baseline at 340 SHP. As the power of the engine was limited by

fuel at higher WFI rates, it is unclear what the relationship would have been between the 1.4 gpm WFI rate and the baseline if the fuel flow rate was not limited.

This investigation also brought to light the many difficulties with the treatment of wet compression. Much more in depth analysis is required than was available to fully characterize the compression process of a liquid/ gas mixture. The assumptions that were made in this investigation were for the purpose of aiding analysis. However, in a robust model of the process, more stringent limits would have to be placed on assumptions. The full investigation would require much more time and effort beyond this project.

This investigation also led to determinations about the applicability of WFI for small gas turbine engines. First, WFI is well suited to decrease the magnitude of nitrous oxide emissions from the engine. WFI is also well suited to increase the net power of the engine. However, both of these effects come at the penalty of decreased thermal efficiency, as represented by Brake specific Fuel Consumption. One would have to determine if improving engine performance with respect to emissions and net power were worth the cost of the slightly increased fuel requirements. It took a lower WFI rate to achieve the effects on the NO_x emissions than it did to achieve significant improvements in net power. In light of this, one would also have to determine if the potential improvements of WFI were worth the cost of the additional volume and weight of the required water. At the 1.4 gpm WFI rate, the 30 gallon tank used in the test was emptied in 20 minutes. Those 30 gallons of water would weigh about 240 lbs. This could severely limit the utility of WFI on a mobile application, such as a helicopter. However, in a stationary application, as long as large enough quantities of clean water were available, Water Fog Injection's improvements of a small gas turbine engine could well be worth the costs.

VI. Recommendations

There are many recommendations on how to further this investigation and what future research would be useful. They are:

- Better understand the effects of and control for the atmospheric conditions
- Adjust test matrix to account for the bleed air valve operation
- Enable better control of fuel supply and make comparisons
- Improve the spray system design such that it is more controllable
- Improve the spray system such that the droplet sizes are consistent and smaller
- Develop or determine an effective way to measure the size of the water droplets
- Calibrate the exhaust gas analyzer and replace if necessary
- Investigate a spray of a water/ biofuel mixture and other types of fuel blends such as JP5-Fisher Tropshe
- Investigate wet compression

Bibliography

1. Urbach, Herman B. et al.. "The Reduction of NOx Emissions from Marine Power Plants." *Proceedings of the Air& Waste Management Association's 90th Meeting &Exhibition.* Toronto: Air & Waste Management Association, Jun 8-13, 1997.

2. Chaker, M., Meher-Homji, C.B. and Mee T.R., III, 2002, "Inlet Fogging of Gas Turbine Engines- Part I: Fog Droplet Thermodynamics, Heat Transfer, and Practical Considerations," Journal of Engineering for Gas Turbines and Power, Vol. 126, pp. 545-558.

3. "Model 250turboshaft." *Rolls-Royce.* 2006. Rolls-Royce. < http://www.rolls-royce.com/defence_aerospace/downloads/helicopters/model250_turboshaft.pdf>, accessed on 16 Feb. 2007

4. General Electric Corporation, Aviation Division, Undated Commercial Literature, <http://www.geae.com/engines/marine/lm2500.html>, accessed 04 September 2007.

5. General Electric Corporation, Aviation Division, "GE'sLM2500 Aeroderivative Gas Turbine Selected for Holland America Line Cruise Ship," Press Release, 8 March 2000, <http://www.geae.com/aboutgeae/presscenter/marine/marine_20000308.html>, accessed 04 September 2007.

Appendix A: WynDyn Calibration File

Channel	Name	Coefficient	Offset
7	Air 1	1.0	0
12	Air 2	1.0	0
1	AirT-V	1.0	0
4	Aux1	0.4096	0
5	Aux2	0.4096	0
76	Baro P	8.0079	0
71	Ch71	75.9250	0
54	CO	0.9816	0
55	CO2	1.9633	0
60	CombP2	37.7537	792
61	CompLw	41.2536	3511
48	CompP1	37.4373	1633
10	DynSpd	1.0	0
2	DynTrq	465.3634	3288
50	Exh LF	37.7892	1597
47	Exh LR	37.6168	1644
52	Exh RF	37.8783	1640
51	Exh RR	91.3857	1640
8	Fuel 1	1.0	0
66	Fuel AF	41.2536	3740
62	Fuel BF	41.2536	3574
11	GGT	728.1401	0
49	GGT P	37.7449	1650
53	HC	981.5386	0
6	HumSen	1.0	0
45	Keil L	75.3130	1500
59	Keil R	75.3836	761
57	NOx	490.8184	0
56	O2	2.4541	0
67	Oil P	41.2536	3634
58	OilFlw	3.4063	0
69	PAMB	2.7503	16945
65	PESL1	16.5016	1920
68	PEXL2	16.5016	16343
63	PEXR1	16.5016	16253
64	PEXR2	16.5016	16358
46	Pres46	38.5272	1622
70	Pres70	2.7503	16246
72	Prs 72	1.0002	0
9	Pwr T	475.5700	0
73	ServoV	-24.4142	0

Appendix B: Engineering Equation Solver Analysis Code

```
"State 1: Initial Conditions"

{P[1]=14.6 [psia]}
{T[1]=(87.7+460) [F]}
{phi[1]=0.296}
{omega[1]=0.001}
{Pv[1]=omega1*Pa[1]/0.622}
phi[1]=(omega*P1)/((0.622+omega)*Pg[1])


Pg[1]=pressure(steam, T=T1, x=0)
Pv[1]=phi[1]*Pg[1]
P1=Pa[1]+Pv[1]

ma_dot=m_dot_air
{mv_dot=1}

omega=mv_dot/ma_dot
mm_dot=ma_dot+mv_dot
mf_a=ma_dot/mm_dot
mf_v=mv_dot/mm_dot

MM_air=MolarMass(Air)
MM_water=MolarMass(water)
MM_m=1/((mf_a/MM_air)+(mf_v/MM_water))
R_u=1.9858 [Btu/lbmol-R]
R_m=R_u/MM_m


"Initial Density of Air and water vapor"
{Vol_dot[1]=2499.9*convert(ft^3/min, ft^3/s)
Vol_dot[1]=Vol_dot_a[1]+Vol_dot_v[1]
Vol_dot_a[1]=ma_dot/rho_a[1]
Vol_dot_v[1]=mv_dot/rho_v[1]
rho_a[1]=P1/(Ra*(T1))
rho_v[1]=P1/(Rv*(T1))
Ra=0.3704
Rv=0.5956 }
{Flow_rate=0.3 [gal/min]}
Vol_dot_w=Flow_rate*1/convert(min,s)*convert(gal, ft^3)
density_water=Density(Water,P=(tank_pressure),x=0)
mv_dot=Vol_dot_w*density_water
{tank_pressure=33.5 [psia]}

sa[1]=entropy(air, T=T1, P=P1)
sv[1]=entropy(steam, T=T1,x=0)
sm[1]=(sa[1]*ma_dot+sv[1]*mv_dot)/mm_dot

ha[1]=enthalpy(air, T=T1)
hv[1]=enthalpy(steam, T=T1, x=0)
hm[1]=(ha[1]*ma_dot+hv[1]*mv_dot)/mm_dot
```

Appendix B: Engineering Equation Solver Analysis Code

```
{h[1]=enthalpy(airh2o, T=T1, w=omega1, P=P1)
h0=enthalpy(air, T=0)
hr[1]=h[1]+h0}

"Compression"
r_p=P2/P1

{Pg[2]=pressure(steam, T=T2, x=1)}
omega=0.622*(Pv[2]/Pa[2])
P2=Pa[2]+Pv[2]
{phi[2]=Pv[2]/Pg[2]}


hm[2]=(ha[2]*ma_dot+hv[2]*mv_dot)/mm_dot
ha[2]=enthalpy(air, T=T2)
hv[2]=enthalpy(steam, T=T2, P=Pv[2])

sa[2]=entropy(air, T=T2, P=Pa[2])
sv[2]=entropy(steam, T=T2, P=Pv[2])
sm[2]=(sa[2]*ma_dot+sv[2]*mv_dot)/mm_dot

sms[2]=sm[1]
sms[2]=(sas[2]*ma_dot+svs[2]*mv_dot)/mm_dot
sas[2]-sa[1]=cp_avg_air*ln((T2s)/(T1))-R_air*ln(Pa[2]/P1)
svs[2]-sv[1]=cp_avg_steam*ln((T2s)/(T1))-R_steam*ln(Pv[2]/Pv[1])

cp_avg_air=0.240 [Btu/lbm-R]
R_air=0.06855 [Btu/lbm-R]

cp_avg_steam=0.445 [Btu/lbm-R]
R_steam=0.1102 [Btu/lbm-R]


{sas[2]=entropy(air, T=T2s, P=P2)
svs[2]=entropy(steam, T=T2s, P=Pv[2])}

hms[2]=(has[2]*ma_dot+hvs[2]*mv_dot)/mm_dot
has[2]=enthalpy(air, P=P2, s=sas[2])
hvs[2]=enthalpy(steam, s=svs[2], P=Pv[2])

{eta_c=0.7104}
eta_c=(hms[2]-hm[1])/(hm[2]-hm[1])


w_c=hm[2]-hm[1]

"State 3:  Constant Pressure Heat Addition"
{T[3]=(1934+460) [F]}

{P[3]=P[2]}
P3=P3_ring
omega=0.622*(Pv[3]/(P3-Pv[3]))
```

Appendix B: Engineering Equation Solver Analysis Code

```
P3=Pa[3]+Pv[3]

ha[3]=enthalpy(air, T=T3)
hv[3]=enthalpy(steam, T=T3, P=Pv[3])
hm[3]=(ha[3]*ma_dot+hv[3]*mv_dot)/mm_dot

sa[3]=entropy(air, T=T3, P=P3)
sv[3]=entropy(steam, T=T3, P=Pv[3])
sm[3]=(sa[3]*ma_dot+sv[3]*mv_dot)/mm_dot


"State 4: Expansion through the gas generator turbine"
{w_ggt=w_c}
w_ggt=hm[3]-hm[4]

omega=(0.622*Pv[4])/(P4-Pv[4])
P4=Pa[4]+Pv[4]

ha[4]=enthalpy(air, T=T4)
hv[4]=enthalpy(steam, T=T4, P=Pv[4])
hm[4]=(ha[4]*ma_dot+hv[4]*mv_dot)/mm_dot

sa[4]=entropy(air, T=T4, P=P4)
sv[4]=entropy(steam, T=T4, P=Pv[4])
sm[4]=(sa[4]*ma_dot+sv[4]*mv_dot)/mm_dot

sms[4]=sm[3]
sms[4]=(sas[4]*ma_dot+svs[4]*mv_dot)/mm_dot
{sas[4]=entropy(air, T=Ts[4], P=P[4])}
sas[4]-sa[3]=cp_avg_air*ln((T4s)/(T3))-R_air*ln(P4/P3)          "From the Gibbs equation"
{svs[4]=entropy(steam, T=Ts[4], P=Pv[4])}
svs[4]-sv[3]=cp_avg_steam*ln((T4s)/(T3))-R_steam*ln(Pv[4]/Pv[3])

{eta_ggt=0.8267}
eta_ggt=(hm[4]-hm[3])/(hms[4]-hm[3])

hms[4]=(has[4]*ma_dot+hvs[4]*mv_dot)/mm_dot
has[4]=enthalpy(air, P=P4, s=sas[4])
hvs[4]=enthalpy(steam, s=svs[4], P=Pv[4])


"State 5: Expansion through the power turbine"
{P[5]=P[1]}
P5=Pa[5]+Pv[5]
omega=(0.622*Pv[5])/(P5-Pv[5])

sms[5]=sm[4]
sms[5]=(sas[5]*ma_dot+svs[5]*mv_dot)/mm_dot
{sas[5]=entropy(air, T=T5s, P=P5)}
sas[5]-sa[4]=cp_avg_air*ln((T5s)/(T4))-R_air*ln(P5/P4)
{svs[5]=entropy(steam, T=Ts[5], P=Pv[5])}
svs[5]-sv[4]=cp_avg_steam*ln((T5s)/(T4))-R_steam*ln(Pv[5]/Pv[4])
```

Appendix B: Engineering Equation Solver Analysis Code

```
hms[5]=(has[5]*ma_dot+hvs[5]*mv_dot)/mm_dot
has[5]=enthalpy(air, P=P5, s=sas[5])
hvs[5]=enthalpy(steam, s=svs[5], P=Pv[5])

{eta_pt=0.989}
eta_pt=(hm[5]-hm[4])/(hms[5]-hm[4])

ha[5]=enthalpy(air, T=T5)
hv[5]=enthalpy(steam, T=T5, P=Pv[5])
hm[5]=(ha[5]*ma_dot+hv[5]*mv_dot)/mm_dot

w_pt=hm[4]-hm[5]

sa[5]=entropy(air, T=T5, P=P5)
sv[5]=entropy(steam, T=T5, P=Pv[5])
sm[5]=(sa[5]*ma_dot+sv[5]*mv_dot)/mm_dot

"Performance Parameters"
q_in=hm[3]-hm[2]
w_net=w_pt

eta_th=w_net/q_in

W_dot_net=mm_dot*w_net
W_dot_net_hp=W_dot_net*convert(Btu/s,hp)


D_inlet=4.5 [in]
A_inlet_inches=3.14*(D_inlet/2)^2
A_inlet=A_inlet_inches*convert(in^2, ft^2)
m_dot_air=rho_1*A_inlet*v_avg_1
rho_1=density(air, T=T1, P=Pa[1])

"This is where I try figuring out the density and water flow stuff with the gas mixture of air and water."
mv_dot=rho_v_1*A_inlet*v_water_avg_1
rho_v_1=density(water, T=T1, P=Pv[1])
c_1v=soundspeed(water, T=T1, P=Pv[1])
Ma_water_1=v_water_avg_1/c_1v

Theta_01=T01/Tref
Tref=518.89 [R]
T01=T1+(v_avg_1^2)*convert(ft^2/s^2, Btu/lbm)/(2*c_p_1)
c_p_1=Cp(Air, T=T1)

delta_01=P01/P_ref
P_ref=14.696 [psia]
P01/P1=(T01/T1)^(k_1/(k_1-1))
k_1=c_p_1/c_v_1
c_v_1=Cv(Air, T=T1)

c_1=SoundSpeed(Air,T=T1)
Ma_1=v_avg_1/c_1
```

Appendix B: Engineering Equation Solver Analysis Code

```
m_dot_c=m_dot_air*((theta_01)^(1/2))/delta_01
{m_dot_fuel=1}

A_airscroll_single_inches=2.0824
A_airscroll_single=A_airscroll_single_inches*convert(in^2,ft^2)
A_airscroll=2*A_airscroll_single
m_dot_air=rho_2*A_airscroll*v_avg_2
rho_2=density(air, T=T2, P=Pa[2])

c_2=SoundSpeed(Air,T=T2)
Ma_2=v_avg_2/c_2

mv_dot=rho_v_2*A_airscroll*v_water_avg_2
rho_v_2=density(water, T=T2, P=Pv[2])
c_2v=soundspeed(water, T=T2, P=Pv[2])
Ma_water_2=v_water_avg_2/c_2v

T02=T2+(v_avg_2^2)*convert(ft^2/s^2, Btu/lbm)/(2*c_p_2)
c_p_2=Cp(Air, T=T2)

P02/P2=(T02/T2)^(k_2/(k_2-1))
k_2=c_p_2/c_v_2
c_v_2=Cv(Air, T=T2)

r_p_total=P02/P01

c_3=SoundSpeed(air, T=T3)
v_avg_3=c_3*Ma_3
rho_3=density(air, T=T3, P=Pa[3])
A_combustor=pi*((6.0625^2-4.25^2))*convert(in^2, ft^2)
m_dot_air=rho_3*A_combustor*v_avg_3

mv_dot=rho_v_3*A_combustor*v_water_avg_3
rho_v_3=density(water, T=T3, P=Pv[3])
c_3v=soundspeed(water, T=T3, P=Pv[3])
Ma_water_3=v_water_avg_3/c_3v

T03=T3+(v_avg_3^2)*convert(ft^2/s^2, Btu/lbm)/(2*c_p_3)
c_p_3=Cp(Air, T=T3)

P03/P3=(T03/T3)^(k_3/(k_3-1))
k_3=c_p_3/c_v_3
c_v_3=Cv(Air, T=T3)

c_4=SoundSpeed(air, T=T4)
v_avg_4=c_4*Ma_4
rho_4=density(air, T=T4, P=Pa[4])
A_powerturbine=pi*(6.0625^2-4.3195^2)*convert(in^2, ft^2)  "For this area I have the difference between the inside and outside radii, but I don't have the absolute radii, so I assumed that the outside radius of the power turbine was the same as the outside radius of the combustor for now.  I will go back and get a better measurement."
m_dot_air=rho_4*A_powerturbine*v_avg_4
```

Appendix B: Engineering Equation Solver Analysis Code

```
mv_dot=rho_v_4*A_powerturbine*v_water_avg_4
rho_v_4=density(water, T=T4, P=Pv[4])
c_4v=soundspeed(water, T=T4, P=Pv[4])
Ma_water_4=v_water_avg_4/c_4v

T04=T4+(v_avg_4^2)*convert(ft^2/s^2, Btu/lbm)/(2*c_p_4)
c_p_4=Cp(Air, T=T4)

P04/P4=(T04/T4)^(k_4/(k_4-1))
k_4=c_p_4/c_v_4
c_v_4=Cv(Air, T=T4)

A_exhaust_single=pi*(7/2)*(4.5/2) [in^2]        "This is the area of the exhaust stack at the point where the pressure sensors and thermocouples are."
A_exhaust=A_exhaust_single*2*convert(in^2, ft^2)
m_dot_air=rho_5*A_powerturbine*v_avg_5
rho_5=density(air, T=T5, P=Pa[5])

mv_dot=rho_v_5*A_powerturbine*v_water_avg_5
rho_v_5=density(water, T=T5, P=Pv[5])
c_5v=soundspeed(water, T=T5, P=Pv[5])
Ma_water_5=v_water_avg_5/c_5v

c_5=SoundSpeed(Air,T=T5)
Ma_5=v_avg_5/c_5

T05=T5+(v_avg_5^2)*convert(ft^2/s^2, Btu/lbm)/(2*c_p_5)
c_p_5=Cp(Air, T=T5)

c_p_v_5=Cp(water, T=T5, P=Pv[5])

P05/P5=(T05/T5)^(k_5/(k_5-1))
k_5=c_p_5/c_v_5
c_v_5=Cv(Air, T=T5)

c_v_v_5=Cv(water, T=T5, P=Pv[5])

rho_m_5=P5/(R_m*T5)*(1/convert(Btu, psia-ft^3))
mm_dot=rho_m_5*A_powerturbine*v_m_avg_5
c_v_m_5=mf_a*c_v_5+mf_v*c_v_v_5
c_p_m_5=mf_a*c_p_5+mf_v*c_p_v_5
k_m_5=c_p_m_5/c_v_m_5

c_5_m=sqrt(k_m_5*R_m*T5*convert(Btu/lbm, ft^2/s^2))
Ma_5_m=v_m_avg_5/c_5_m

r_p_pt=P04/P05
r_p_ggt=P03/P04

T2_sat=T_sat(Water,P=P2)
```

Appendix C: Standard Operating Procedures for the Model 250-C20B

To start the engine:

1. Turn on computer.
2. Ensure fuel pump is on and there is fuel pressure
3. Ensure the battery is charged and the power to the dynamometer and control system is turned on.
4. Ensure the water for the water brake is on. Valve should be fully open.
5. Check the turbine oil level.
6. Ensure that the Louvers are open.
7. Check that the fan grating is clear.
8. Turn on exhaust fan.
9. Turn on power at the control bench.
10. Open WinDyn computer program.
11. Place engine control knob to 30%, manual, and med adjustment setting
12. Set dynamometer brake speed to 6000 rpm, and med adjustment setting
13. In WinDyn, select “turbine1” or “turbine2”
14. Turn on Ignition
15. Turn on starter, and hold in.
16. When Gas Generator Turbine speed is at 14,000 rpm, turn on fuel pump. Keep “GGT Temperature” below 1415 F.
17. When GGT speed is 25,000 rpm, turn off starter and ignition.
18. Allow engine to “warm up” for a minute or two before beginning runs.

To stop the engine:

1. Slowly bring engine back down to idle (30% control knob setting)
2. Allow engine to cool off at this setting for a minute or so.
3. Turn off fuel pump.
4. Place engine control knob on 0%.
5. Turn off computer.
6. Turn off fan.
7. Close louvers.
8. Turn off water.
9. Turn off power.
10. Turn off fuel pumps.

Appendix D: Droplet in Compressor Heat Transfer Analysis

Assumptions:

- T_{inf} is the average temperature of the compressor inlet and compressor discharge
- $T_{droplet}$ is constant and equal to room temperature
- The pressure of the environment is the average pressure of the compressor inlet and compressor discharge.
- The velocity of the flow through the compressor is the average of the velocity at the compressor inlet and the compressor discharge.
- The droplet diameter does not change. It is 50 μm.
- Assumed a lumped system analysis. The work for this is done below in Part #1.

$$D = 50\mu m = 1.6404x10^{-4}\ ft$$

$$T_{\inf} = \frac{T_2 + T_1}{2} = \frac{942.67R + 523.17R}{2} = 732.9R = 272.9°F$$

$$T_{Drop} = 532R = 72°F$$

$$P = \frac{P_1 + P_2}{2} = \frac{102.6\,psia + 14.7\,psia}{2} = 58.656\,psia$$

Background:

To determine if the droplet would vaporize by the time it exits the compressor, it is determined if the droplet spends enough time in the compressor to gain enough energy to change phase. To make this determination, the amount of heat transfer needed to change the phase of the droplet is estimated. The heat transfer rate for the system was also estimated. The comparison of these two characteristics allows one to estimate how much time is needed to transfer enough energy to the droplet to make it change phase. Based on the speed of the air flow through the compressor, the amount of time that the droplet spends in the compressor was estimated. (It was also assumed that the water droplet would remain a droplet through out the length of the compressor, which is not entirely accurate.)

$$\Delta Q_{req} = \Delta Q_{sensible} + \Delta Q_{latent}$$

$$\Delta Q_{req} = m_{drop} c_{p,drop} \Delta T + m_{drop} h_{fg}$$

$$\frac{\Delta Q}{\Delta t} = \frac{dQ}{dt} = q$$

Part #1: Can it be assumed that the temperature is uniform across the droplet?

Is Bi≤0.1?

Appendix D

$$Bi = \frac{hL_c}{k}$$

$$L_c = \frac{Vol}{A_s} = \frac{\frac{4}{3}\pi\left(\frac{D}{2}\right)^3}{4\pi\left(\frac{D}{2}\right)^2} = \frac{D}{6} = \frac{1.6404x10^{-4}\ ft}{6} = 2.734x10^{-5}\ ft$$

$$k_{H_2O}\left(T = 72°F\right) = 0.347\frac{Btu}{hftR}$$

$$Bi = \frac{h\left(2.734x10^{-4}\ ft\right)}{0.347\frac{Btu}{hftR}}$$

$$Bi = 7.879x10^{-5}h$$

So what h do I use? The limiting h is determined below.

$$0.01 = 7.879x10^{-5}h$$

$$h = 126.92\frac{Btu}{h - ft^2 - R}$$

If the heat transfer coefficient is lower than 126.9 then the assumption of a lumped system is valid.

Part#2: What is the heat transfer rate?

$$q = \bar{h}A_s\left(T_s - T_\infty\right)$$

Error! Bookmark not defined.

$$A_s = 4\pi\left(\frac{D}{2}\right)^2 = 8.4538x10^{-8}\ ft^2$$

The question now is what heat transfer coefficient should be used. There are two ways to consider the environment of the droplet in the air. The first is that the droplet and the surrounding air travel through the compressor at the same tangential velocity. This means the relative velocity between the droplet and the surrounding air is 0 ft/s. This would be the equivalent of a natural convection system.

The second limiting case would be to consider the maximum possible relative velocity between the droplet and the surrounding air. This would be equivalent to the droplet being stationary in surrounding air. This could be considered an external forced convection system.

It is assumed that the average heat transfer coefficient for the system would be somewhere between the two.

Appendix D

a) The natural convection case:
The expression for the average Nusselt number comes from p.511 of *Heat and Mass Transfer* by Çengle.

$$\overline{Nu} = \frac{\bar{h}L}{k}$$

$$\overline{Nu} = 2 + \frac{0.589\, Ra_D^{1/4}}{\left[1 + \left(0.469/\Pr\right)^{9/16}\right]^{4/9}}$$

$$\Pr\left(T = 272\,^\circ F\right) = 0.705208$$

$$Ra_D = Gr_D \Pr = \frac{g\beta\left(T_s - T_\infty\right)L^3}{\nu^2}\Pr$$

$$g = 32.2\left(\frac{ft}{s}\right)^2$$

$$\nu\left(T_\infty, P_{avg}\right) = 0.71871\ x10^{-4}\ \frac{ft^2}{s}$$

$$L = D$$

$$\beta = \frac{1}{T_\infty} = \frac{1}{732.9R} = 0.001364\ \frac{1}{R}$$

$$Ra_D = \frac{\left[32.2\left(ft/s\right)^2\right]\left(0.001364\ \frac{1}{R}\right)\left(732.9R - 532\,R\right)\left(1.6404\ x10^{-4}\ ft\right)^3}{\left(0.71871\ x10^{-4}\ ft^2/s\right)^2}\left(0.705208\right)$$

$$Ra_D = 0.005294$$

$$\overline{Nu} = 2 + \frac{\left(0.589\right)\left(0.005294\right)^{1/4}}{\left[1 + \left(0.469/0.705208\right)^{9/16}\right]^{4/9}}$$

$$\overline{Nu} = 2.1225$$

$$\overline{Nu} = \frac{hD}{k}$$

$$k_{air,T_\infty} = 0.019228\ \frac{Btu}{h - ft - R}$$

$$\overline{Nu} = 2.1225 = \frac{h\left(1.6404\ x10^{-4}\ ft\right)}{0.019228\ \frac{Btu}{h - ft - R}}$$

$$\bar{h} = 248.8\,\frac{Btu}{h - ft^2 - R}$$

Appendix D

b) The External Forced Convection over a sphere. In this case, the droplet is assumed to be stationary and the air stream velocity at the average air stream velocity, v_{avg}.

$$|\vec{v}|_1 = 433.9 \; ft/s$$

$$|\vec{v}|_2 = 417.6 \; ft/s$$

$$|\vec{v}|_{avg} = \frac{|\vec{v}|_1 + |\vec{v}|_2}{2} = 425.75 \; ft/s$$

The following correlation for the Nusselt number is from p. 413 of *Heat and Mass Transfer* by Çengle.

$$\overline{Nu}_D = \frac{hD}{k} = 2 + \left[0.4\,\mathrm{Re}^{1/2} + 0.06\,\mathrm{Re}^{2/3} \right] \mathrm{Pr}^{0.4} \left(\frac{\mu_\infty}{\mu_s} \right)^{1/4}$$

$$\mathrm{Re}_D = \frac{|\vec{v}|_{avg} D}{\nu} = \frac{\left(425.75 \; ft/s \right)\left(1.6404 x 10^{-4} \; ft \right)}{5.5805 x 10^{-5} \; ft^2/s} = 971.7$$

$$\mathrm{Pr} = 0.705208$$

$$\mu_\infty = 1.557 x 10^{-5} \; lbm/ft - s$$

$$\mu_s = 1.23 x 10^{-5} \; lbm/ft - s$$

$$\overline{Nu}_{sphere} = 2 + \left[0.4(971.7)^{1/2} + 0.06(971.7)^{2/3} \right] (0.705208)^{0.4} \left(\frac{1.557 x 10^{-5}}{1.23 x 10^{-5}} \right)^{1/4}$$

$$\overline{Nu}_{sphere} = \frac{\bar{h} D}{k} = \frac{\bar{h}\left(1.6404 x 10^{-4} \; ft \right)}{0.019228 \frac{Btu}{h - ft - R}} = 18.9309$$

$$\bar{h} = 2218.99 \frac{Btu}{h - ft^2 - R}$$

Appendix D

Part#3: How much energy must be transferred to a droplet for it to change phase?

$$\Delta Q_{required} = m_{droplet}\, c_{p,H_2O}\left(T_{sat} - T_1\right) + m_{droplet}\, h_{fg,H_2O}$$

$$\Delta Q_{required} = m_{droplet}\left[c_{p,H_2O}\left(T_{sat} - T_1\right) + h_{fg,H_2O}\right]$$

$$m = \rho V$$

$$V = \frac{4}{3}\pi\left(\frac{D}{2}\right)^3 = \frac{4}{3}\pi\left(\frac{1.6404\,x10^{-4}}{2}\right)^3 = 2.3113\,x10^{-12}\ ft^3$$

$$\rho\left(T = 72°F, P = 14.7\,psia\right) = 62.30\ lbm/ft^3$$

$$m = \left(2.3113\,x10^{-12}\ ft^3\right)\left(62.30\ lbm/ft^3\right) = 144.0x10^{-12}\,lbm$$

$$c_p = 1\frac{Btu}{lbm - R}$$

$$h_{fg} = 1054\ Btu/lbm$$

$$T_{sat}\left(P = 58.9\,psia\right) = 290°F$$

$$\Delta Q_{required} = \left(144.0x10^{-12}\,lbm\right)\left[\left(1\frac{Btu}{lbm - R}\right)\left(290 - 72°F\right) + 1054\ Btu/lbm\right]$$

$$\Delta Q_{required} = 183.17\,x10^{-9}\,Btu$$

Part #4: What is the heat transfer rate for the two cases, and how much time does it take for the droplet to gain enough energy to change to vapor phase in each case?

$$\Delta t = \frac{\Delta Q}{q}$$

Natural Convection case:

$$q_{natural} = \bar{h}_{natural} A_s\left(T_s - T_\infty\right) = \left(248.8\frac{Btu}{h - ft^2 - R}\right)\left(8.454x10^{-8}\ ft^2\right)\left(272.9 - 72°F\right)$$

$$q_{natural} = 4.2066x10^{-3}\frac{Btu}{h}$$

$$\Delta t_{nat.} = \frac{\Delta Q_{req}}{q_{natural}}$$

$$\Delta t_{nat.} = \frac{183.17x10^{-9}\,Btu}{4.2066x10^{-3}\frac{Btu}{h}} = 43.54x10^{-6}\,h\left(\frac{3600s}{h}\right)$$

$$\Delta t_{nat.} = 156.8x10^{-3}\,s = 157ms$$

Appendix D

External Forced Convection case:

$$q_{forced} = \bar{h}_{forced} A_s \left(T_s - T_\infty\right) = \left(2218.99 \frac{Btu}{h - ft^2 - R}\right)\left(8.454x10^{-8}\ ft^2\right)\left(272.9 - 72°F\right)$$

$$q_{forced} = 37.518x10^{-3} \frac{Btu}{h}$$

$$\Delta t_{forced} = \frac{\Delta Q_{req}}{q_{forced}}$$

$$\Delta t_{forced} = \frac{183.17x10^{-9} Btu}{37.518x10^{-3} \frac{Btu}{h}} = 4.88219x10^{-6} h\left(\frac{3600s}{h}\right)$$

$$\Delta t_{forced} = 17.576x10^{-3} s = 17.58ms$$

Part #5: How long does the droplet stay in the compressor?

L is the length of the compressor.

$$\left|\vec{v}\right|_{avg,droplet} = 425.75 \frac{ft}{s}$$

$$L = 1\,ft$$

$$\Delta t = \frac{L}{\left|\vec{v}\right|} = \frac{1\,ft}{425.75 \frac{ft}{s}}$$

$$\Delta t_{compressor} = 2.35ms$$

The time that the droplet is estimated to spend in the compressor is less than the amount of time necessary for the droplet to vaporize in either of the limiting cases.